

1 **Analogue experiments on releasing and restraining bends and their**
2 **application to the study of the Barents Shear Margin**

3
4
5
6 **Roy H. Gabrielsen¹⁾, Panagiotis A. Giannenas²⁾, Dimitrios Sokoutis^{1,3)}, Ernst**
7 **Willingshofer³⁾, Muhammad Hassaan^{1,4)} & Jan Inge Faleide¹⁾**

8
9 ¹⁾ Department of Geosciences, University of Oslo, Norway

10 ²⁾ Univ Rennes, CNRS, Géosciences Rennes, UMR 6118, 35000 Rennes, France

11 ³⁾ Faculty of Geosciences, Utrecht University, the Netherlands

12 ⁴⁾ Vår Energi AS, Grundingen 3, 0250 Oslo, Norway

13
14
15 **Corresponding author: Roy H. Gabrielsen (r.h.gabrielsen@geo.uio.no)**

16
17 **ORCI-id:**

18 Jan Inge Faleide: 0000-0001-8032-2015

19 Roy H. Gabrielsen: 0000-0001-5427-8404

20 Muhammad Hassaan: 0000-0001-6004-8557

21
22
23
24
25 **Abstract:**

26 The Barents Shear Margin separates the Svalbard and Barents Sea from the North
27 Atlantic. During the break-up of the North Atlantic the plate tectonic configuration
28 was characterized by sequential dextral shear, extension, an eventually
29 contraction and inversion. This generated a complex zone of deformation that
30 contains several structural families of over-lapping and reactivated structures.

31 A series of crustal-scale analogue experiments, utilizing a scaled stratified sand-
32 silicon polymer sequence were utilized in the study of the structural evolution of
33 the shear margin.

34
35 The most significant observations of particular significance for interpreting the
36 structural configuration of the Barents Shear Margin are:

37 1) Prominent early-stage positive structural elements (e.g. folds, push-ups)
38 interacted with younger (e.g. inversion) structures and contributed to a hybrid
39 final structural pattern.

40 2) Several structural features that were initiated during the early (dextral shear)
41 stage became overprinted and obliterated in the subsequent stages.

42 3) All master faults, pull-part basins and extensional shear duplexes initiated
43 during the shear stage quickly became linked in the extension stage, generating a
44 connected basin system along the entire shear margin at the stage of maximum
45 extension.

46 4) The fold pattern generated during the terminal stage (contraction/inversion
47 became dominant in the basin areas and was characterized by fold axes striking
48 parallel to the basin margins. These folds, however, strongly affected the shallow
49 intra-basin layers.

50 The experiments reproduced the geometry and positions of the major basins and
51 relations between structural elements (fault and fold systems) as observed along
52 and adjacent to the Barents Shear Margin. This supports the present structural
53 model for the shear margin.

54
55

56 **Plain language summary:**

57 The Barents Shear Margin defines the border between the relatively shallow
58 Barents Sea that is situated on a continental plate, and the deep ocean. The margin
59 is characterized by a complex structural pattern that has resulted from the
60 opening and separation of the continent and the ocean, starting c. 65 million years
61 ago. This history included on phase of right-lateral shear and one phase of
62 spreading, the latter including a sub-phase of shortening, perhaps due to plate
63 tectonic reorganizations. The area has been mapped by the study of reflection
64 seismic lines for decades, but many details of its development is not yet fully
65 constrained. We therefore ran a set of scaled experiments to investigate what kind
66 of structures could be expected in this kind of tectonic environment, and to figure
67 out what is a reasonable time relation between them. From these experiments we
68 deduced several types of structures (faults, folds and sedimentary basins) that
69 help us to improve the understanding of the history of the opening of the North
70 Atlantic.

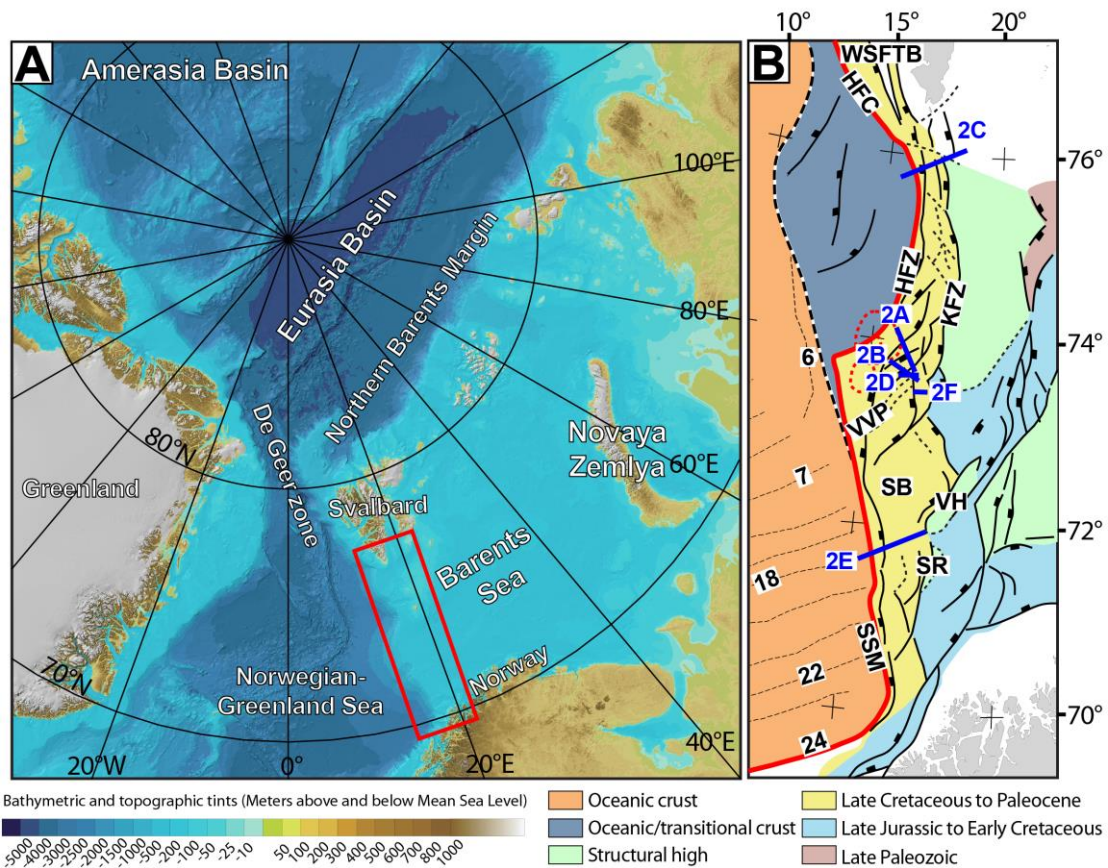
71
72
73

74 **Key words:** Analogue experiments, dextral strike-slip, releasing and restraining
75 bends, multiple folding, Barents Shear Margin, basin inversion

76
77

78 **Introduction**

79
80 Physiography, width and structural style of the Norwegian continental margin
81 vary considerably along its strike (e.g. Faleide et al., 2008, 2015). The margin
82 includes a southern rifted segment between 60° and 70°N and a northern sheared-
83 rifted segment between 70° and 82°N (**Figure 1A**). The latter coincides with the
84 ocean-ward border of the western Barents Sea and Svalbard margins (e.g. Faleide
85 et al., 2008) and is referred to here as “the Barents Shear Margin”. This segment
86 coincides with the continent-ocean transition (COT) of the northernmost part of
87 the North Atlantic Ocean, and its configuration is typical for that of transform
88 margins where the structural pattern became established in an early stage of
89 shear, later to develop into an active continent-ocean passive margin (Mascle &
90 Blarez, 1987; Lorenzo, 1997; Seiler et al., 2010; Basile, 2015; Nemcok et al., 2016).
91 Late Cretaceous - Palaeocene shear, rifting, breakup and incipient spreading in the
92 North Atlantic was associated with voluminous magmatic activity, resulting in the
93 development of the North Atlantic Volcanic Province (Saunders et al., 1997;
94 Ganerød et al., 2010; Horni, 2017). According to its tectonic development, the
95 Barents Shear Margin (**Figure 1B**) incorporates, or is bordered by, several distinct
96 structural elements, some of which are associated with volcanism and halokinesis.
97 The multistage development combined with a complex geometry caused
98 interference between structures (and sediment systems) in different stages of the
99 margin development. Such relations are not always obvious, but interpretation
100 can be supported by the help of scale-models. We combine the interpretation of
101 reflection seismic data and analogue modeling. Thus, we investigate structures
102 generated in (initial) dextral shear. These were generated during initial dextral
103 shear the development into seafloor spreading and subsequent contraction. The
104 later stages (contraction) were likely influenced by plate reorganization (Talwani
105 & Eldholm, 1977; Gaina et al., 2009; see also Våagnes et al., 1998; Pascal &
106 Gabrielsen, 2001; Pascal et al., 2005; Gac et al., 2016) or other far-field stresses
107 (Doré & Lundin, 1996; Lundin & Doré, 1997; Doré et al., 1999; 2016; Lundin et al.,
108 2013). The present experiments were designed to illuminate the structural
109 complexity affiliated with multistage sheared passive margins, so that the
110 significance of structural elements like fault and fold systems observed along the
111 Barents Shear Margin could be set into a dynamic context. The study area suffered



112

113 **Figure 1: A)** The Barents Sea is separated from the Norwegian-Greenland Sea by
 114 the de Geer transfer margin. Red box shows the present study area. **B)** Structural
 115 map Barents Sea shear margin. Note segmentation of the continent-ocean
 116 transition. Abbreviations (from north to south): WSFTB = West Spitsbergen Fold-
 117 and-Thrust Belt, HFZ = Hornsund Fault Complex, KFC = Knølegga Fault Zone, VVP
 118 = Vestbakken Volcanic Province, SB = Sørvestsnaget Basin, VH = Veslemøy High,
 119 SR = Senja Ridge, SSM = Senja Shear Margin. Blue lines indicate position of seismic
 120 profiles in Figure 2 and red line X-X' shows western border of thinned crust (see
 121 also Figure 3). Chron numbers are indicated on oceanic crust area.

122

123 repeated and contrasting stages of deformation, including dextral shear, oblique
 124 extension, inversion and volcanic activity. This is a particular challenge in such
 125 tectonic settings that are characterized by repeated overprinting and
 126 cannibalization of younger structural elements. Results from the he experiments
 127 facilitate the identification and characterization of structural elements at the
 128 different stages of deformation and to identify the structural elements that were
 129 developed at stages of deformation preceding the present-day margin
 130 configuration.

131

132

133 **Regional background**

134 In the following sections we provide definitions and a short description of the
135 main structural elements constituting the study area. The structural elements are
136 presented in-sequence from north to south (**Figure 1B**).

137 The greater **Barents Shear Margin** is a part of the more extensive De Geer
138 Zone mega shear system which linked the Norwegian Greenland Sea and the Arctic
139 Eurasia system (Eldholm et al., 1987; 2002; Faleide et al., 1988; Breivik et al.,
140 1998; 2003). Together with its conjugate Greenland counterpart it carries the
141 evidence of post-Caledonian extension that culminated with Cenozoic break-up of
142 the North Atlantic (e.g. Brekke, 2000; Gabrielsen et al., 1990; Faleide et al., 1993;
143 Gudlaugsson et al., 1998). Two shear margin segments are separated by a central
144 rift-dominated segment along the Barents Shear Margin (Myhre et al., 1982;
145 Vågnes, 1997; Myhre & Eldholm, 1988; Ryseth et al., 2003; Faleide at al., 1988;
146 1993; 2008). Each segment maintained the structural and magmatic
147 characteristics of the crust during its development. Of these the Senja Shear
148 Margin is the southernmost segment, originally termed the Senja Fracture Zone
149 by Eldholm et al. (1987). Here NNW-SSE-striking folds interfere with NE-SW-
150 striking structures (Giannenas, 2018). Strain partitioning characterizes the shear
151 zone system (e.g. West Spitsbergen; Leever et al., 2011a,b and the Sørvestsnaget
152 Basin; Kristensen et al., 2017).

153

154 **The Hornsund Fault Zone and West Spitsbergen Fold-and Thrust Belt** form
155 the northernmost segment of the Barents Shear Margin. It coincides with the
156 southern continuation of the De Geer Zone and the Senja Shear Margin. The
157 Hornsund Fault Zone belongs to this system and provides a type setting for
158 transpression and strain partitioning together with the West Spitsbergen fold-
159 and-thrust-belt (Harland, 1965; 1969; 1971; Lowell, 1972; Gabrielsen et al., 1992;
160 Maher et al., 1997; Leever et al., 2011 a,b). Plate tectonic reconstructions suggest
161 that the plate boundary accommodated c. 750 km along-strike dextral
162 displacement and 20-40 km of shortening in the Eocene (Bergh et al., 1997; Gaina
163 et al., 2009).

164

165 **The Knølegga Fault Zone** can be seen as a part of the Hornsund fault system
166 extending from the southern tip of Spitsbergen (Gabrielsen et al., 1990). It trends
167 NNE-SSW to N-S and defines the western margin of the Stappen High. The vertical
168 displacement approaches 6 km. Although the main movements along the fault may
169 be Tertiary of age, it is likely that it was initiated much earlier. The Tertiary
170 displacement may have a lateral (dextral) component (Gabrielsen et al., 1990).

171

172 **The Vestbakken Volcanic Province** is the main topic of this contribution. It
173 represents the central rifted segment of the Barents Shear Margin and links the
174 sheared margin segments to the north and south occupying a right-double
175 stepping (eastward) releasing-bend-setting. Prominent volcanoes and sill-
176 intrusions suggest three distinct volcanic events in the Vestbakken Volcanic
177 Province (Jebsen & Faleide, 1998; Faleide et al., 2008; Libak et al., 2012). It is
178 constrained to its east by the eastern boundary fault (EBF in **Figure 1B**), that is a
179 part of the Knølegga Fault Complex, separating the Vestbakken Volcanic Province
180 from the marginal Stappen High to the east. To the south and southeast the
181 Vestbakken Volcanic Province drops gradually towards the Sørvestsnaget Basin
182 across the southern extension of the eastern boundary fault and its associated
183 faults. To the west and north the area is delineated by the continent – ocean
184 boundary/transition. The Vestbakken Volcanic Province includes both
185 extensional and contractional structures (e.g. Jebsen & Faleide, 1998; Faleide et
186 al., 2008; Blaich et al., 2017). Two main episodes of Cenozoic extensional faulting
187 were identified in the Vestbakken Volcanic Province: (i) a late Paleocene-early
188 Eocene event, which correlates in time with the continental break-up in the
189 Norwegian-Greenland Sea, (ii) an early Oligocene event that is tentatively
190 correlated to plate reorganization around 34 Ma activating NE-SW striking faults.
191 Volcanic activity coincides with these events.

192

193 **The Sørvestsnaget Basin** occupies the area east the COT between 71 and 73°N
194 and is characterized by an exceptionally thick Cretaceous-Cenozoic sequence
195 (Gabrielsen et al., 1990). To the west it is delineated by the Senja Shear Margin
196 and to the northeast it is separated from the Bjørnøya Basin by the southern part
197 of the Knølegga Fault Complex (Faleide et al., 1988). The position of the Senja

198 Ridge coincides with southeastern border of the Sørvestsnaget Basin (Figure 1B),
199 whereas the Vestbakken Volcanic Province is situated to its north. An episode of
200 Cretaceous rifting in the Sørvestsnaget Basin climaxed in the Cenomanian-middle
201 Turonian (Breivik et al., 1998), succeeded by Late Cretaceous-Palaeocene fast
202 sedimentation (Ryseth et al., 2003). Particularly the later stages of the basin
203 formation were strongly influenced by the opening of the North Atlantic (Hanisch,
204 1984; Brekke & Riis, 1987). Salt diapirism also contributed to the development of
205 this basin (Perez-Garcia et al., 2013).

206

207 **The Senja Ridge** (SR in **Figure 1B**) runs parallel to the continental margin and
208 coincides with the western border of the Tromsø Basin. It is characterized by a N-
209 S-trending gravity anomaly which are interpreted as buried mafic-ultramafic
210 intrusions which are associated with the Seiland Igneous Province (Fichler &
211 Pastore, 2022). The structural development of the Senja Ridge has been associated
212 with shear affiliated with the development of the shear margin (Riis et al., 1986)
213 and though it was a positive structural element from the mid Cretaceous to the
214 Pliocene it may have been activated at an even earlier stage (Gabrielsen et al.,
215 1990).

216

217 **The Senja Shear Margin** was active during the Eocene opening of the Norwegian-
218 Greenland Sea dextral shear causing splitting out of slivers of continental crust.
219 These slivers became embedded in the oceanic crust during continued seafloor
220 spreading (Faleide et al., 2008). The Senja Shear Margin coincides with the
221 western margin of a basin system superimposed on an area of significant crustal
222 thinning. This part of the shear margin was characterized by a composite
223 architecture even at the earliest stages of its development (Faleide et al., 2008).
224 The basin system accumulated sedimentary sequences that reached thicknesses
225 of up to 18-20 km. Subsequent shearing contributed to the development of
226 releasing and restraining bends, associated pull-apart-basins, neutral strike-slip
227 segments, flower-structures and fold-systems (*sensu* Crowell, 1974 a,b; Biddle &
228 Christie-Blick, 1985a,b; Cunningham & Mann, 2007a,b). Particularly the hanging
229 wall west of the Knølegga Fault Complex (see below) of the Barents Shear Margin
230 was affected by wrench deformation as seen from several push-ups and fold

231 systems (Grogan et al., 1999; Bergh & Grogan 2003). The structural development
232 of the margin was complicated by active halokinesis (Knutsen & Larsen, 1997;
233 Gudlaugsson et al., 1998; Ryseth et al., 2003).

234

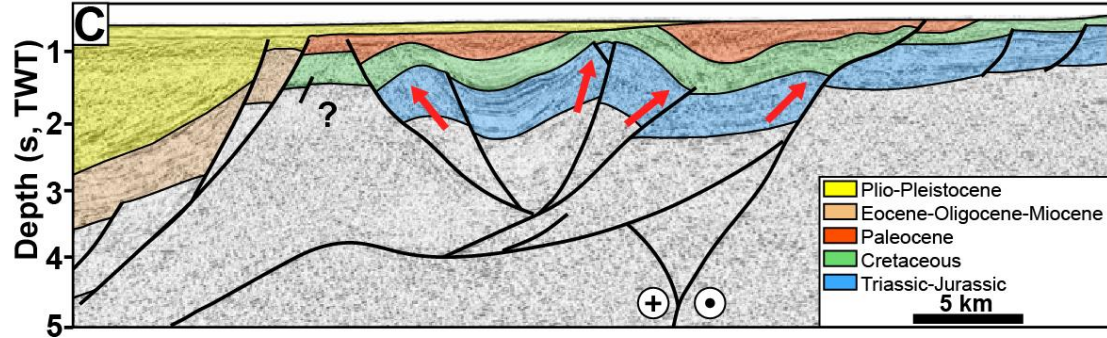
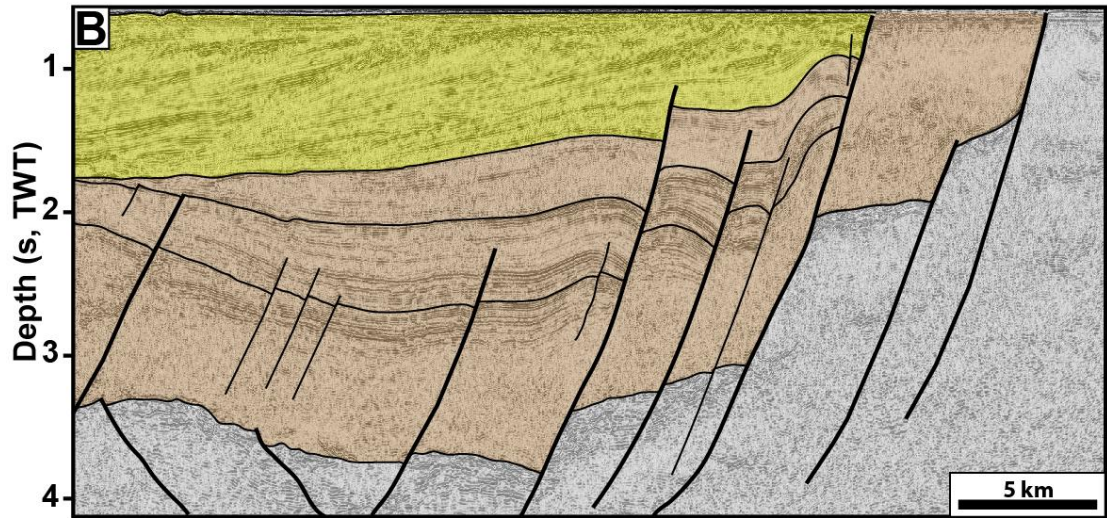
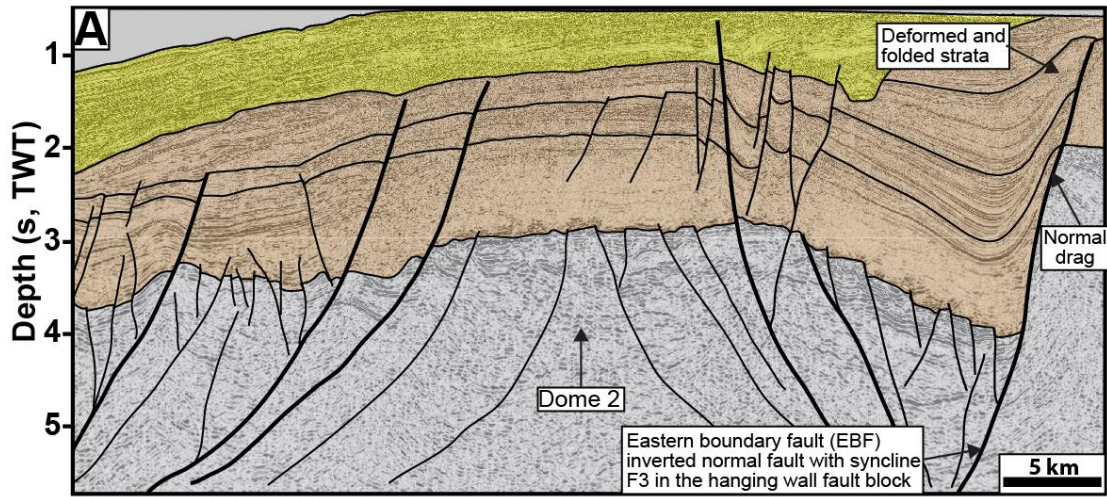
235 **Reflection seismic data and structural interpretation**

236 The data set of this study includes 2D seismic reflection data from several surveys and
237 well data in the Vestbakken Volcanic Province. Data coverage is less dense in northern
238 part of the study area. Typical spacing of seismic lines is 4 km. Well 7316/5-1 was used
239 to correlate the seismic data with formation tops in the study area whereas published
240 paper based correlations provided calibration and age of each seismic horizon mapped
241 (e.g. Eidvin et al., 1993; 1998 Ryseth et al., 2003). Three stratigraphic groups are
242 encountered in the well, namely the Nordland Group (between 473 - 945 m); the
243 Sotbakken Group (between 945-3752m) and Nygrunnen Group (between 3752-4014m)
244 (Eidvin et al., 1993; 1998; www.npd.com). Several folds of regional significance and
245 with axial traces that can be followed along strike for 2-3 km or more occur in the
246 Vestbakken Volcanic Province. The folds commonly are situated in the hanging walls
247 of extensional faults and the fold traces and the structural grain of the thick-skinned
248 master faults are generally parallel. This shows that the position and orientation of the
249 folds were determined by the preexisting basement structural fabric. The mapping of
250 the folds is constrained by the spacing of reflection seismic lines, so each fold trace may
251 include undetected overlap-zones or axial off-sets. The folds were identified on the
252 lower Eocene, Oligocene and lower Miocene levels. All the mapped folds are either
253 positioned in the hanging walls of extensional (sometimes inverted) master faults or are
254 dissected by younger faults with minor throws.

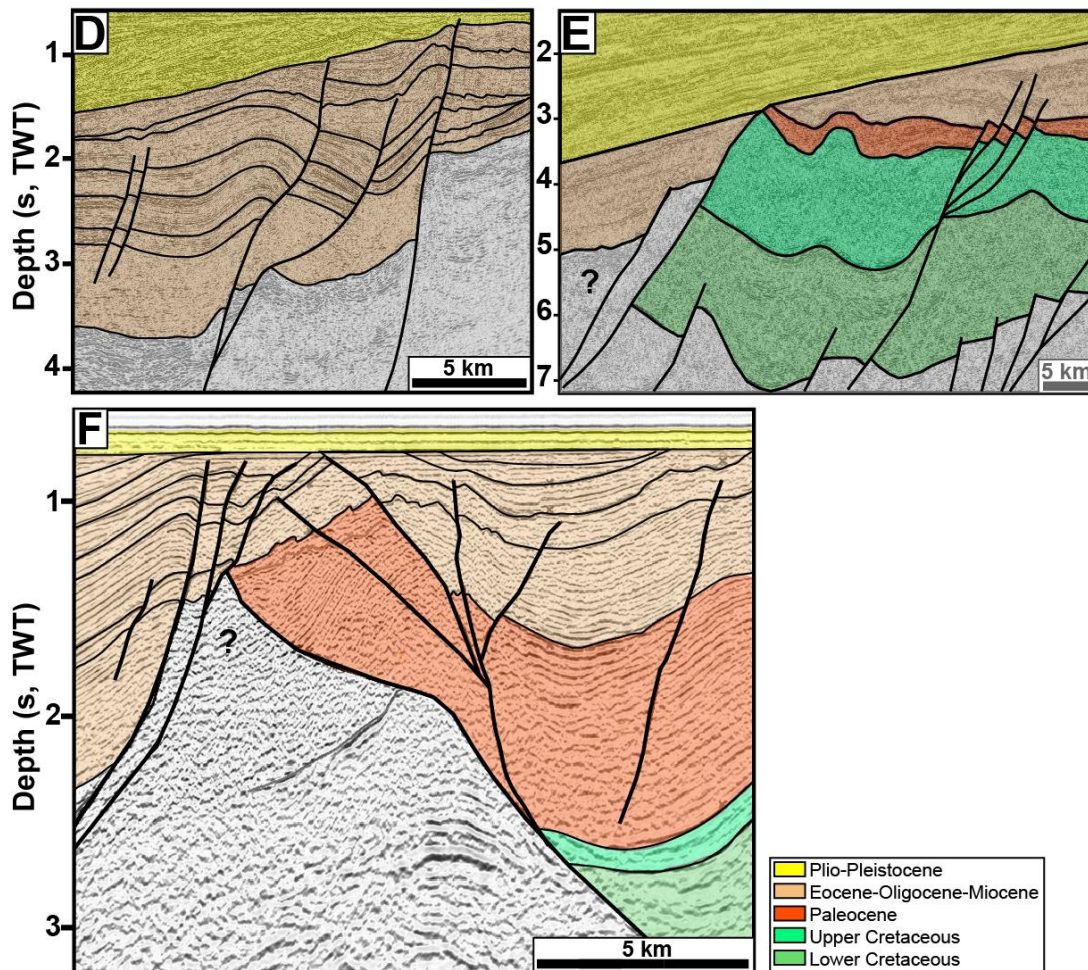
255

256 **Strike-slip systems and analogue shear experiments**

257 Shear margins and strike-slip systems are structurally complex and highly
258 dynamic, so that the eventual architecture of such systems include structural
259 elements that were not contemporaneous (e.g. Graymer et al., 2007; Crowell,
260 1962; 1974a,b; Woodcock & Fischer, 1986; Mousloupoulou et al., 2007; 2008).
261 Analogue models offer the option to study the dynamics of such relations and
262 therefore attracted the attention of early workers in this field (e.g. Cloos, 1928;
263 Riedel, 1929) and have continued to do so until today. Early experimental works



264
 265
 266
 267
 268
 269
 270
 271
 272



273

274 **Figure 2:** Seismic examples, Vestbakken Volcanic Province. **A)** Gentle, partly
 275 collapsed NE-SW-striking anticline/dome of uncertain origin in the eastern
 276 terrace domain of the southern Vestbakken Volcanic Province. **B,C)** Asymmetrical
 277 folds (fold family 2; Giannenas 2018) situated along the eastern margin of the
 278 Vestbakken Volcanic Province. These may represent primary SPE-4-structures
 279 focused in the hanging walls along margins of master fault blocks, representing
 280 reactivated SPE-2-structures. **D)** trains of symmetrical folds with upright fold axes
 281 (corresponding to PSE-5-structures) are preserved inside larger fault blocks. See
 282 text for explanation of SPE-structures. **E)** Section through push-up associated with
 283 restraining bend (PSE-4-structure). **F)** Flower (PSE-2)-structure in area
 284 dominated by neutral shear.

285

286 mostly utilized one-layer (“Riedel-box”) models (e.g. Emmons, 1969; Tchalenko,
 287 1970; Wilcox et al., 1973), which were soon to be expanded by the study of
 288 multilayer systems (e.g. Faugère et al., 1986; Naylor et al., 1986; Richard et al.,
 289 1991; Richard & Cobbold, 1989, 1995; Schreurs, 1994, 2003; Manduit & Dauteuil,
 290 1996; Dateuil & Mart, 1998; Schreurs & Colletta, 1998, 2003; Ueta et al., 2000;
 291 Dooley & Schreurs, 2012). The systematics and dynamics of strike-slip systems
 292 have been focused upon in a number of summaries like Sylvester (1985; 1988);

293 Biddle & Christie-Blick (1985 a,b); Cunningham & Mann (2007); Dooley &
294 Schreurs (2012); Nemcok et al. (2016) and Peacock et al. (2016). Concepts and
295 nomenclature established in these works are used in the following descriptions
296 and analysis. Also, following Christie-Blick & Biddle (1985a,b) and Dooley &
297 Schreurs (2012) we apply the term Principal Deformation Zone (PDZ) for the
298 junction between the movable polythene plates underlying the experiment. The
299 contact between the fixed and movable base defined a non-stationary velocity
300 discontinuity (“VD”; Ballard et al., 1987; Allemand & Brun, 1991; Tron & Brun,
301 1991).

302 Several experimental works have particularly focused on the geometry and
303 development of pull-apart-basins in releasing bend settings (Mann et al., 1983;
304 Faugère et al., 1983; Richard et al., 1995; Dooley & McClay, 1997; Basile & Brun,
305 1999; Sims et al., 1999; Le Calvez & Vendeville, 2002; Mann, 2007; Mitra & Paul,
306 2011). The pull-apart basin was described by Burchfiel & Stewart (1966) and
307 Crowell (1974a,b) as formed at a releasing bend or at a releasing fault step-over
308 along a strike-slip zone (Biddle & Christie-Blick, 1985a,b). This basin type has also
309 been termed “rhomb grabens” (Freund, 1971) and “strike-slip basins” (Mann et
310 al., 1993) and is commonly considered to be synonymous with the extensional
311 strike-slip duplex (Woodcock & Fischer, 1986; Dooley & Schreurs, 2012). In the
312 descriptions of our experiments, we found it convenient to distinguish between
313 extensional strike-slip duplexes in the context of Woodcock & Fischer (1986) and
314 Twiss & Moores (2007, p. 140-141) and pull-apart basins (rhomb grabens:
315 Crowell, 1974 a,b; Aydin & Nur, 1993) since they reflect slightly different stages in
316 the development in our experiments (see discussion).

317

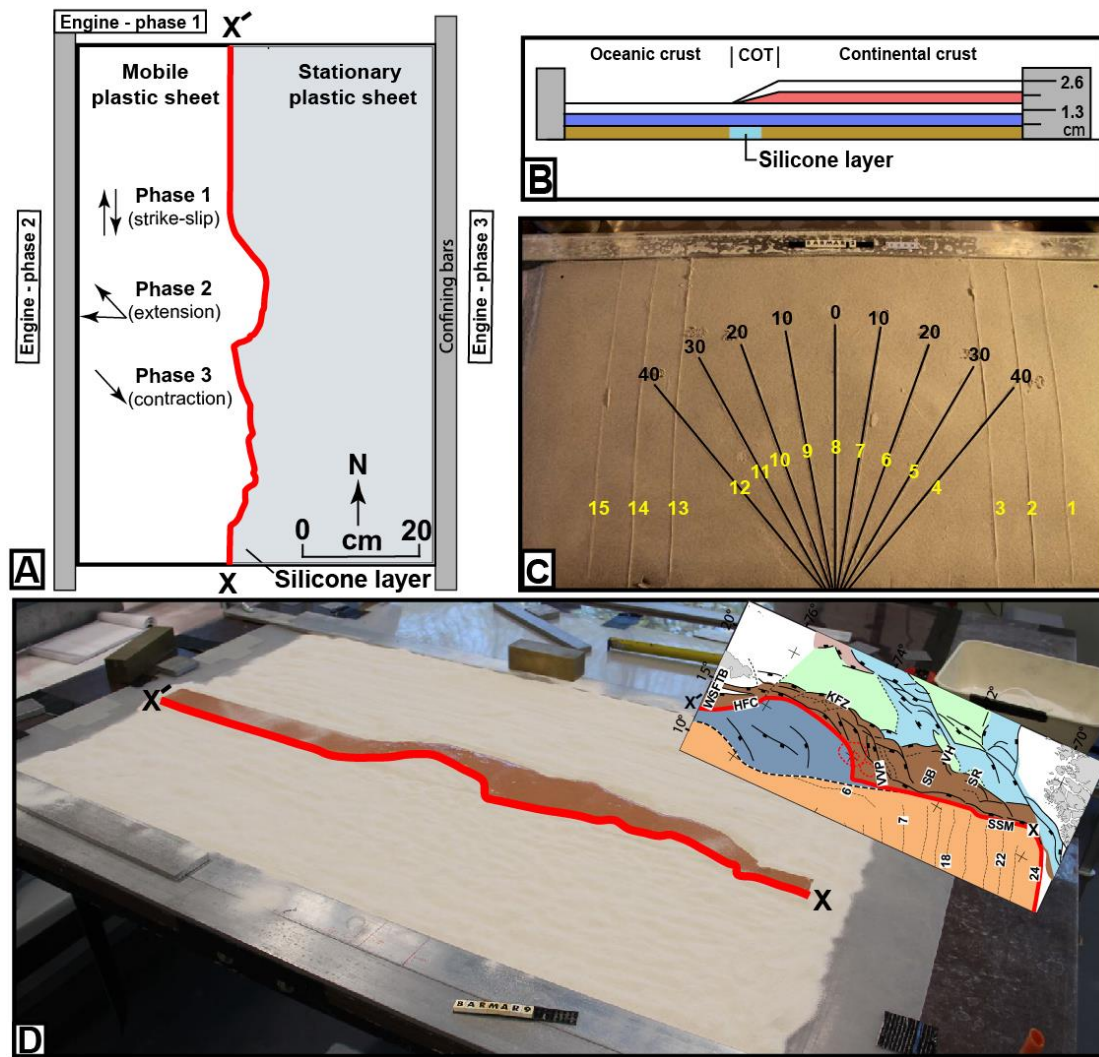
318 **Experimental setup**

319 To study the kinematics of complex shear margins, a series of analogue
320 experiments were performed at the tectonic modelling laboratory (TecLab) of
321 Utrecht University, The Netherlands. All experiments were built on two
322 overlapping 1 mm thick plastic sheets (each 100 cm long and 50 cm wide) that
323 were placed on a flat, horizontal table surface. The boundary between the
324 underlying movable and overlying stationary plastic sheets had the shape of the
325 mapped continent-ocean boundary (COB; **Figure 1B**). The moveable sheet was

326 connected to an electronic engine, which pulled the sheet at constant velocity
327 during all three deformation stages. Displacement rates were therefore not scaled.
328 The modelling material was then placed on these sheets where the layers on the
329 stationary sheet represent the continental crust including the continent-ocean
330 transition (COT) whereas those on the mobile sheet represents the oceanic crust.
331 The model layers were confined by aluminum bars along the long sides and sand
332 along the short sides (**Figure 3A**). The continental crust tapers off towards the
333 oceanic crust with a relatively constant gradient. A sand-wedge with a constant
334 dip angle determined by the difference in thickness between the intact and the
335 stretched crust, and that covered the width of the silicon putty layer, was made to
336 simulate the ocean-continent transition (**Figure 3B**). The taper angle was kept
337 constant for all models.

338 The pre-cut shape of the plate boundary includes major releasing bends
339 positioned so that they correspond to the geometry of the COB and the three main
340 structural segments of the Barents Shear Margin as follows. *Segment 1* of the
341 BarMar-experiments (**Figure 4**) contained several sub-segments with releasing
342 and restraining bends as well as segments of “neutral” (Wilcox et al., 1973; Mann
343 et al. 1983; Biddle & Christie-Blick, 1985b) or “pure” (Richard et al., 1991) strike-
344 slip. *Segment 2* had a basic crescent shape, thereby defining a releasing bend at its
345 southern margin in the position similar to that of the Vestbakken Volcanic
346 Province that merged into a neutral shear-segment along the strike of, whereas a
347 restraining bend occupied the northern margin of the segment. *Segment 3* was a
348 straight basement segment, defining a zone of neutral shear and corresponds to
349 the strike-slip segment west of Svalbard (**Figure 1**).

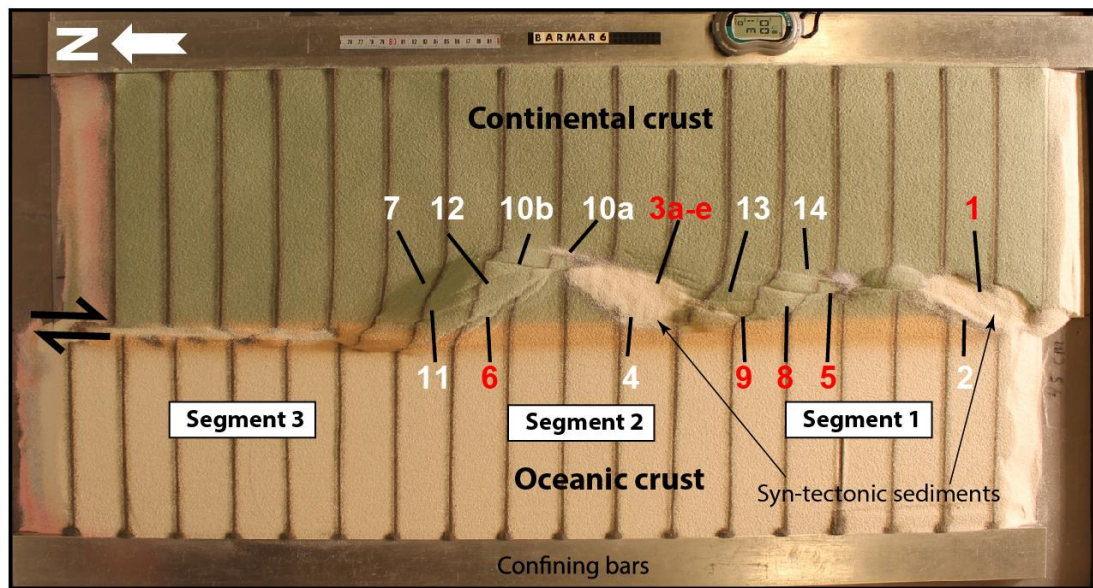
350 The experiments included three stages of deformation with constant rates
351 of movement of the mobile sheet at 10 cmhr^{-1} in all three stages. The relative
352 angles of plate movements in the experiments were taken from post late
353 Paleocene opening directions in the northeast Atlantic (Gaina et al., 2009). Dextral
354 shear was applied in the *first phase* in all experiments by pulling the lower plastic
355 sheet by 5 cm. In the *second phase* the left side of the experiment was extended by
356 3 cm orthogonally (BarMar6) or obliquely (315 degrees; BarMar 8 & 9) to the
357 trend of the shear margin, whereas plate motion was reversed during the *third*
358 *phase of deformation*, leading to inversion of earlier formed basins that had been



359

360 **Figure 3:** A) Schematical set-up of BarMar3-experiment as seen in map view. B)
 361 Section through same experiment before deformation, indicating stratification
 362 and thickness relations. C) Standard positions and orientation for sections cut in
 363 all experiments in the BarMar-series. Yellow numbers are section numbers. Black
 364 numbers indicate angle between the margins of the experiment (relative to N-S)
 365 for each profile. D) Outline of silicone putty layer as applied in all experiments.
 366 Inset shows original structural map of the Barents Margin used to define the width
 367 of the thinned crust. Red line (X-X') indicates the western limit of the thinned zone.
 368

369 developed in the strike-slip and extensional phases. Sedimentary basins that
 370 develop due to strike-slip (phase 1) or extension (phase 2) have been filled with
 371 layers of colored feldspar sand by sieving, so that a smooth surface was obtained.
 372 These layers are primarily important for discriminating among deformation
 373 phases and thus act as marker horizons. Phase 3 was initiated by inverting the
 374 orthogonal (BarMar6) or oblique (BarMar 8 & 9) extension of Phase 2 to
 375 contraction as a proxy for ridge-push that likely was initiated when the mid-



376

377 **Figure 4:** Position of segments and major structural elements as referred to in the
 378 text and subsequent figures (see particularly **Figures 5 and 6**). This example is
 379 taken from the reference experiment BarMar6. All experiments BarMar6-9
 380 followed the same pattern, and the same nomenclature was used in the
 381 description of all experiments and provides the template for the definition of
 382 structural elements in **Figure 7**.

383

384 oceanic ridge was established in Miocene time in the North Atlantic (Moser et al.,
 385 2002; Gaina et al., 2009). Contraction generated by ridge-push has been inferred
 386 from the mid Norwegian continental shelf (Vågnes et al., 1998; Pascal &
 387 Gabrielsen, 2001; Faleide et al., 2008; Gac et al., 2016) and seems still to prevail in
 388 the northern areas of Scandinavia (Pascal et al., 2005), although far-field
 389 compression generated by other processes have been suggested (e.g. Doré &
 390 Lundin, 1996).

391 Coloured layers of dry feldspar sand represent the brittle oceanic and
 392 continental crust. This material has proven suitable for simulating brittle
 393 deformation conditions (Willingshofer et al., 2005; Luth et al., 2010; Auzemery et
 394 al., 2021). It is characterized by a grain size of 100-200 μm , a density of 1300 kgm^{-3} ,
 395 a cohesion of $\sim 16\text{-}45$ Pa and a peak friction coefficient of 0.67 (Willingshofer et
 396 al., 2018). Additionally, a 8 mm thick and of variable width corresponding to the
 397 transition zone (as mapped in reflection seismic data) of 'Rhodorsil Gomme GSIR'
 398 (Sokoutis, 1987) silicone putty mixed with fillers was used as a proxy for the
 399 thinned and weakened continental crust at the ocean-continent transition (**Figure**

400 **1B and 3A,B**). This Newtonian material ($n=1.09$) has a density of 1330 kgm^{-3} and
401 a viscosity of $1.42 \times 10^4 \text{ Pa.s}$.

402 The experiments were scaled following standard scaling procedures as
403 described by Hubbert (1937), Ramberg (1967) or Weijermars and Schmeling
404 (1986), assuming that inertia forces are negligible when modelling tectonic
405 processes on geologic timescales (see Ramberg (1981) and Del Ventisette et al.
406 (2007) for a discussion on this topic). The models were scaled so that 10 mm in
407 the model approximates c. 10 km in nature yielding a length scale ratio of 1.00×10^{-6} .
408 As such, the model oceanic and continental crusts scale to 18 and 26 km in nature,
409 respectively, which, although slightly overestimating the oceanic crustal thickness
410 (10-12 km) is in full agreement with the estimated thickness of the thinned
411 oceanward segment of the continental crust (30-20 km Breivik et al., 1998).

412 The brittle crust, dry feldspar sand, deforms according to the Mohr-
413 Coulomb fracture criterion (Horsfield, 1977; Mandl et al., 1977; McClay, 1990;
414 Richard et al., 1991; Klinkmüller et al., 2016), whereas silicone putty promotes
415 ductile deformation and folding. The geometry applied in the present experiments
416 is accordingly well suited for the study of the COB in the Barents Shear Margin
417 (Breivik et al., 1998).

418 When complete, the experiments were covered with a thin layer of sand
419 further to stabilize the surface topography before the models were saturated with
420 water and cross-sections that were oriented transverse to the velocity
421 discontinuity were cut in a fan-shaped pattern (**Figure 3C**). All experiments have
422 been monitored with a digital camera providing top-view images at regular time
423 intervals of one minute.

424 All experiments performed were oriented in a N-S-coordinate framework
425 to facilitate comparison with the western Barents Sea area and had a three-stage
426 deformation sequence (dextral shear – extension – contraction). All descriptions
427 and figures relate to this orientation. It was noted that all experiments reproduced
428 comparable basic geometries and structural types, demonstrating robustness
429 against variations in contrasting strength of the “ocean-continent”-transition
430 zone, which included a zone of silicone putty with variable width below an
431 eastward thickening sand-wedge (**Figure 3B**). The experiments were terminated
432 before the full closure of the basin system, in accordance with the extension vector

433 > contraction vector as in the North Atlantic (see Vågnes et al. 1998; Pascal &
434 Gabrielsen 2001; Gaina et al. 2009).

435

436 **Modelling Results**

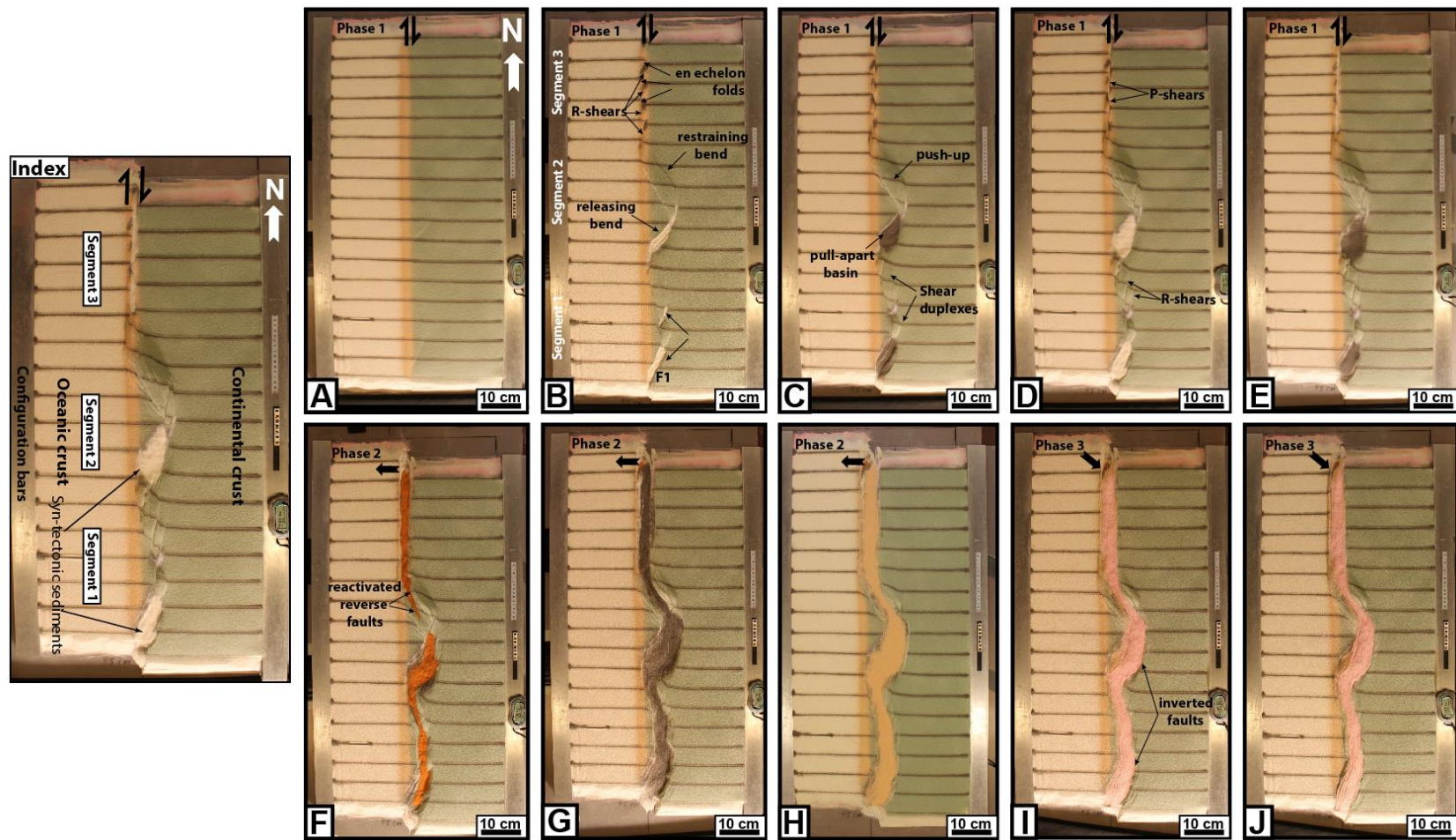
437 A series of nine experiments (BarMar1-9) with the set-up described above was
438 performed. Experiments BarMar1-5 were used to calibrate and optimize
439 geometrical outline, deformation rate, and angles of relative plate movements and
440 are not shown here. The optimized geometries and experimental conditions were
441 utilized for experiments BarMar6-9, of which BarMar6 and 8 (and some examples
442 from BarMar9) are illustrated here. They yielded similar results in that all crucial
443 structural elements (faults and folds) were reproduced in all experiments as
444 described in the text are shown in **Figure 4**. It is emphasized that the extensional
445 basins affiliated with the extension phase (phase 2) were wider for the orthogonal
446 (BarMar6) as compared to the oblique extension experiments (BarMar 8)
447 (**Figures 5 and 6**). Furthermore, the fold systems generated in the experiments
448 that utilized oblique contraction of $315/135^{\circ}$ (BarMar8-9) produced more
449 extensive systems of non-cylindrical folds. These folds also had continuous, but
450 more curved fold traces as compared to the experiments with orthogonal
451 extension/contraction (BarMar6). The fold axes generally rotated to become
452 parallel to the (extensional) master faults delineating the pull-apart basins
453 generated in deformation stage 1 in experiments with an oblique opening/closing
454 angle.

455 Examples of the sequential development is displayed in **Figures 5 and 6**,
456 and summarized in **Figure 7**. Elongated positive structural elements with fold-like
457 morphology as seen on the surface were detected during the various stages of the
458 present experiments. The true nature of those were not easily determined until
459 the experiments were terminated and transects could be examined. Such
460 structures included buried push-ups (*sensu* Dooley & Schreurs, 2012), antiformal
461 stacks, back-thrusts, positive flower structures, fold trains, and simple anticlines.
462 For convenience, we use the non-genetic term “positive structural elements”
463 termed *PSEm-n* for such structure types as seen in the experiments in the
464 following description. In the following the deformation in each segment is
465 characterized for the three deformation phases (**Table 1**).

466 **Table 1**
 467 Characteristics of Positive Structural Element (PSE 1-6) as described in the text and shown in figures. Note that the PSE-1-structures that
 468 were developed in the earliest stages of the experiments became cannibalized during the continued deformation. No candidates of these
 469 structures were identified in the reflection seismic sections.
 470

Struct. type	Structural configuration	Orientation	Expr. stage	Segment	Recognized in seismic	Figure Expr	Figure Seism
PSE-1	Open syn-anticline system	135 deg	Stage 1	1,3	?	5,6	1A?
PSE-2	Incipient flower or half-flower	Parallel master fault	Stage 1	1,2,3	Yes	5,6,8	1B
PSE-3	Forced folds above rotated fault blocks	Parallel master fault in releasing bend	Stage 2	1,2	Yes	9B	
PSE-4	Push-up	Parallel master fault in restraining bend	Stage 1	2	Yes	9D	1C
PSE-5	Anticlines/snake-heads in hanging walls	Parallel master faults	Stage 3	1,2,3	Yes	9C,D	1D,E
PSE-6	Anticline-syncline trains	Parallel master faults	Stage 3	1,2,3	Yes	12	1F

471



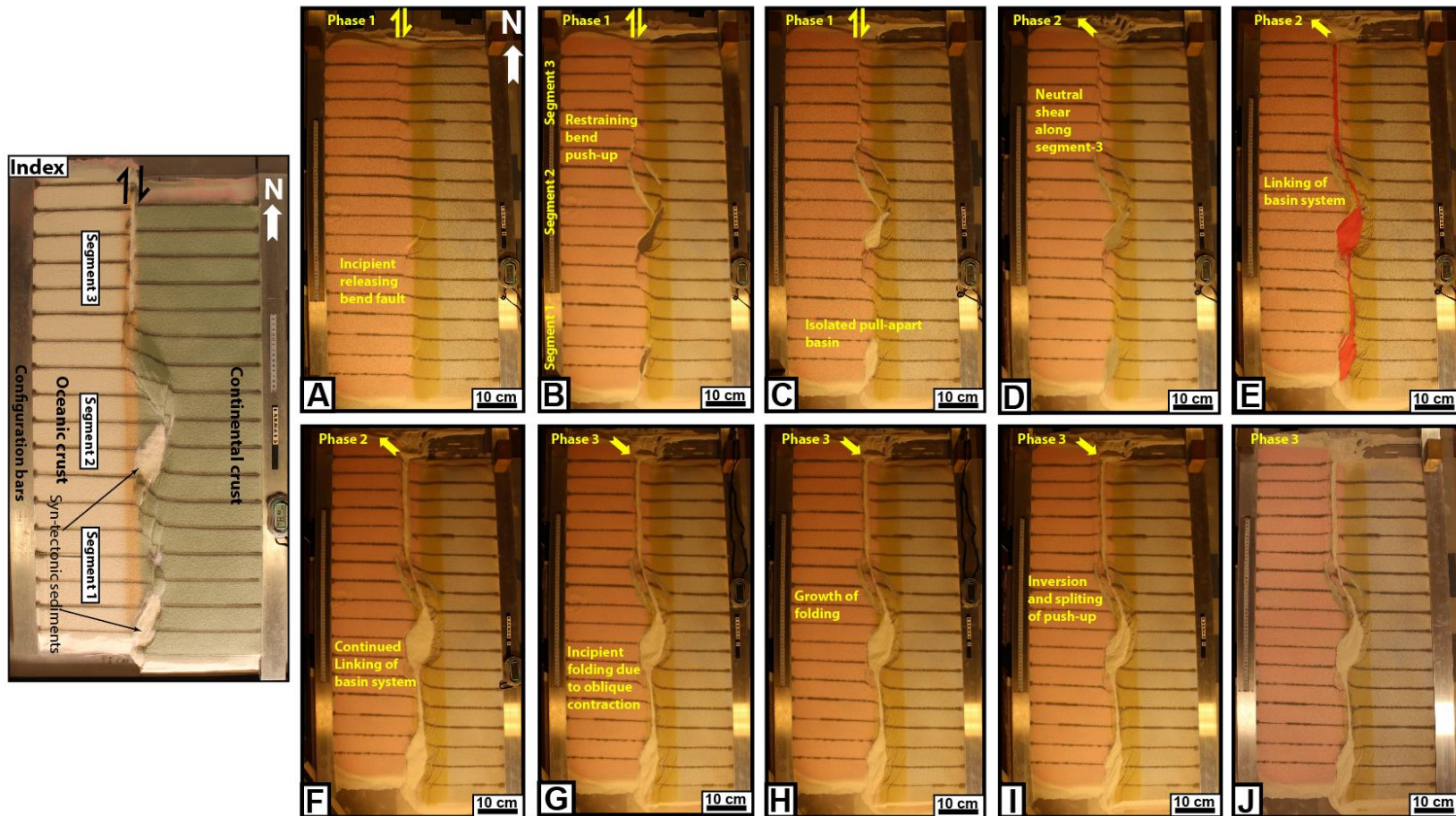
472

473 **Figure 5:** Sequential development of experiment BarMar6 by 0.5, 2.4, 3.5, 4.0 and 5.0 cm of dextral shear (Steps A-E), orthogonal extension
 474 (steps F-H) and oblique contraction (steps I-J). The master fault strands are numbered in **Figure 4**, and the sequential development for
 475 each structural family is shown in **Figure 7**. The reference panel to the upper left shows the positions of the segments.

476 **Deformation phase 1: Dextral shear stage**

477 *Segment 1:* Differences in the geometry of the pre-cut fault trace between
478 segments 1, 2 and 3 became visible after the very initial deformation stage.
479 Particularly in segments 1 and 3 an array of oblique *en échelon* folds in between
480 Riedel shear structures (*PSE-1-structures*) oriented c. 135°(NW-SE) to the regional
481 VD rotating towards NNW-SSE by continued shear (**Figure 8**; see also Wilcox et
482 al., 1973; Ordonne & Vialon, 1983; Richard et al., 1991; Dooley & Schreurs, 2012).
483 These were simple, harmonic folds with upright axial planes and fold axial traces
484 extending a few cm beyond the surface shear-zone described above. They had
485 amplitudes on the scale of a few millimeters and wavelengths on scale of 5 cm. The
486 *PSE-1-structures* interfered with or were dismembered by younger structures (Y-
487 shears and *PSE-2-structures*; see below) causing northerly rotation of individual
488 intra-fault zone lamellae (remnant *PSE-1-structures*; **Figure 8**). Structures similar
489 to *PSE-1-fold* arrays are known from almost all strike-slip experiments reported
490 and described in the literature (e.g. Cloos, 1928; Riedel, 1929; See Dooley &
491 Schreurs, 2012 for summary) and are therefore not given further attention here.
492 By 0.25 cm of horizontal displacement in segment 1, which included releasing and
493 restraining bends separated by a central strand of neutral shear, a slightly
494 curvilinear surface trace of a NE-SW-striking, top-NW normal fault in the
495 southernmost part of segment 1 developed. This co-existed with the *PSE-1-*
496 *structures* and became paralleled by a normal fault with opposite dip (fault 2,
497 **Figure 4**) so that the two faults constrained a crescent- or spindle-shaped
498 incipient extensional shear duplex (**Figures 5B and 6B**; see also Mann et al.,
499 1983).

500 A system of separate *en échelon* N-S to NNE-SSE-striking normal and shear
501 fault segments became visible in segment 1 after ca. 1 cm of shear (**Figure 5C,D**).
502 These faults did not have the orientations as expected for R (Riedel) - and R' (anti-
503 Riedel)- shears (that would be oriented with angles of approximately 15 and 75°
504 from the master fault trace) but became progressively linked with along strike
505 growth and the development of new faults and fault segments. They thereby
506 acquired the characteristics of Y-shears (oriented sub-parallel to the master fault
507 trace), dissecting the *PSE-1-structures*. By 2.4 cm of shear, segment 1 had become
508 one unified fault array (**Figures 5D and 6D**), delineating a system of incipient



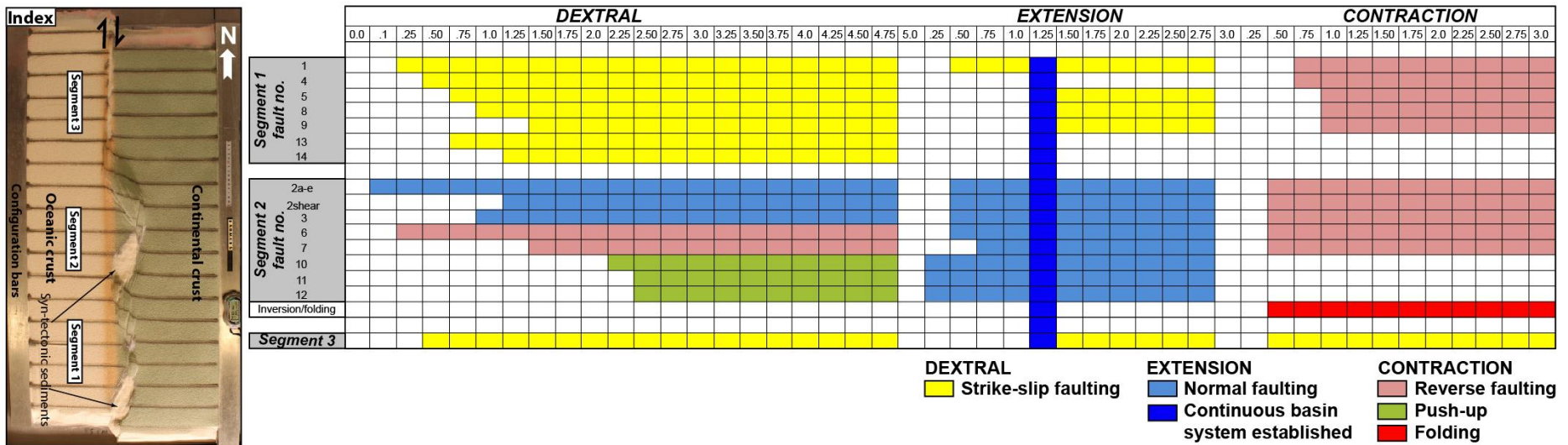
509

510 **Figure 6:** Sequential development of experiment BarMar8 by 0.5, 2.4, 3.5, 4.0 and 5.0 cm of dextral shear (Steps A-E), oblique extension
 511 (steps F-H) and oblique contraction (steps I-J). The master fault strands are numbered in **Figure 3**, and the sequential development for
 512 each structural family is shown in **Figure 7**. Phases 2 and 3 involved oblique (315°) extension and contraction in this experiment. The
 513 reference panel to the upper left shows the positions of the segments.

514 push-ups or positive flower structures (*PSE-2-structures*; **Figures 8 and 10**,
515 **sections B1 and B3**).

516 The PSE-2-structures had amplitudes of 1 - 2 cm and wavelengths of 3 - 5
517 cm as measured on the surface with fault surfaces that steepened down-section,
518 the deepest parts of the structures having cores of sand-layers deformed by open
519 to tight folds. The folds had upright or slightly inclined axial planes, dipping up to
520 55°, mainly to the east. The structures also affected the shallowest layers down to
521 1-2 cm in the sequence, but the shallowest sequences were developed at a later
522 stage of deformation and were characterized by simple gentle to open anticlines.
523 These structures were constrained to a deformation zone directly above the trace
524 of the basement fault, similar to that commonly seen along shear zones (e.g.
525 Tchalenko, 1971; Crowell, 1974 a,b; Dooley & Schreurs, 2012). This zone was 3-4
526 cm wide and remained stable throughout deformation stage 1 and was restricted
527 to the close vicinity of the basement shear fault itself. A horse-tail-like fault array
528 developed by ca. 3 cm of shear at the transitions between segments 1 and 2
529 (**Figures 5B-D and 6B-D**).

530 The structuring in *Segment 2* was ruled by the pre-cut crescent-shaped
531 basement fault (velocity discontinuity) that caused the development of a releasing
532 bend along its southern, and a restraining bend along its northern border (**Figure**
533 **11**). The first fault of fault array 3a-e in the southern part of Segment 2 (**Figure 4**)
534 was activated after c. 0.15 cm of bulk horizontal displacement (**Figure 7**). It was
535 situated directly above the southernmost pre-cut releasing bend, defining the
536 margin of crescent-shaped incipient extensional strike-slip duplexes (in the
537 context of Woodcock & Fischer, 1986, Woodcock & Schubert, 1994 and Twiss &
538 Moores, 2007, p. 140-141). The developing basin got a spindle-shaped structure
539 and developed into a basin with a lazy-S-shape (Cunningham & Mann, 2007; Mann,
540 2007). The basin widened towards the east by stepwise footwall collapse,
541 generating sequentially rotating crescent-shaped extensional fault blocks that
542 became trapped as extensional horses in the footwall of the releasing bend
543 (**Figure 11**). In the areas of the most pronounced extension the crestal part of the
544 rotational fault blocks became elevated above the basin floor, generating ridges
545 that influenced the basin floor topography and hence, the sedimentation. By
546 continued rotation of the fault blocks and simultaneous sieving of sand the crests

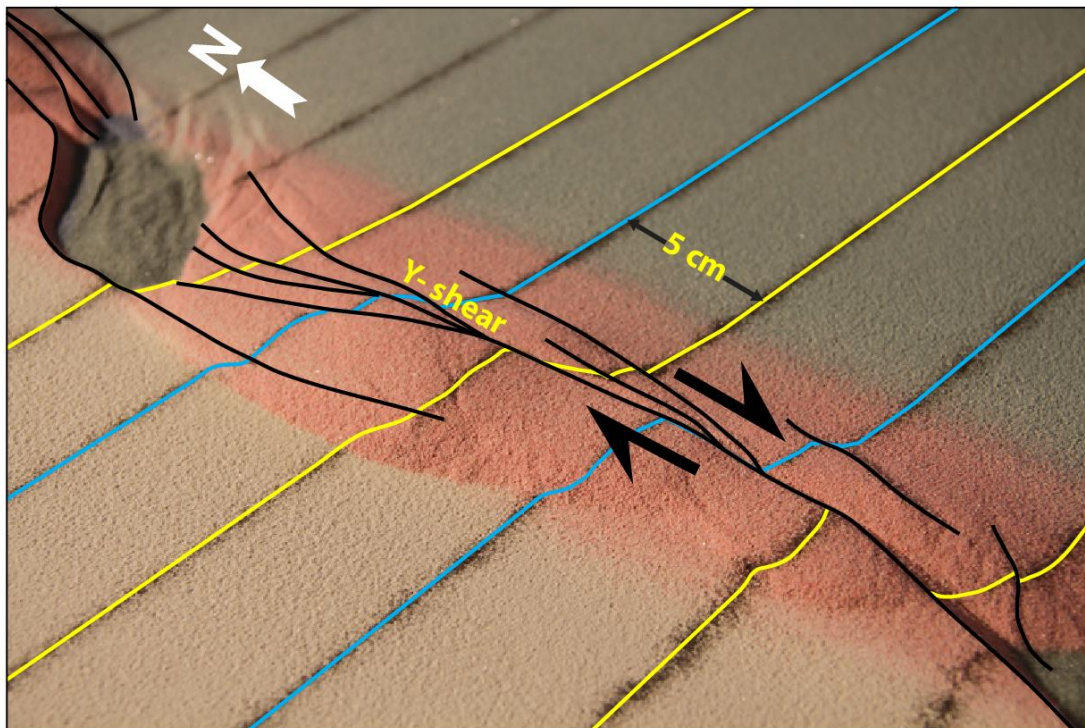


547

548 **Figure 7:** Summary of sequential activity in each master fault in Experiment BarMar6 (**Figure 5**) (for position of each fault, see **Figure 4**).
 549 Type and amount of displacement is shown in two upper horizontal rows. The vertical blue bar indicates the stage at which full along-
 550 strike communication became established between marginal basins. Color code (see in-set) indicates type of displacement at any stage.
 551 The reference panel to the left shows the positions of the segments.

552 of the blocks became sequentially uplifted, generating forced folds (Hamblin,
553 1965; Stearns, 1978; Groshong, 1989; Khalil & McClay, 2016) (**Figure 10A**). In the
554 analysis we used the term *PSE-3-structures* for these features. Simultaneously, an
555 expanding sand-sequence became trapped in the footwalls of the master faults,
556 defining typical growth-fault geometries.

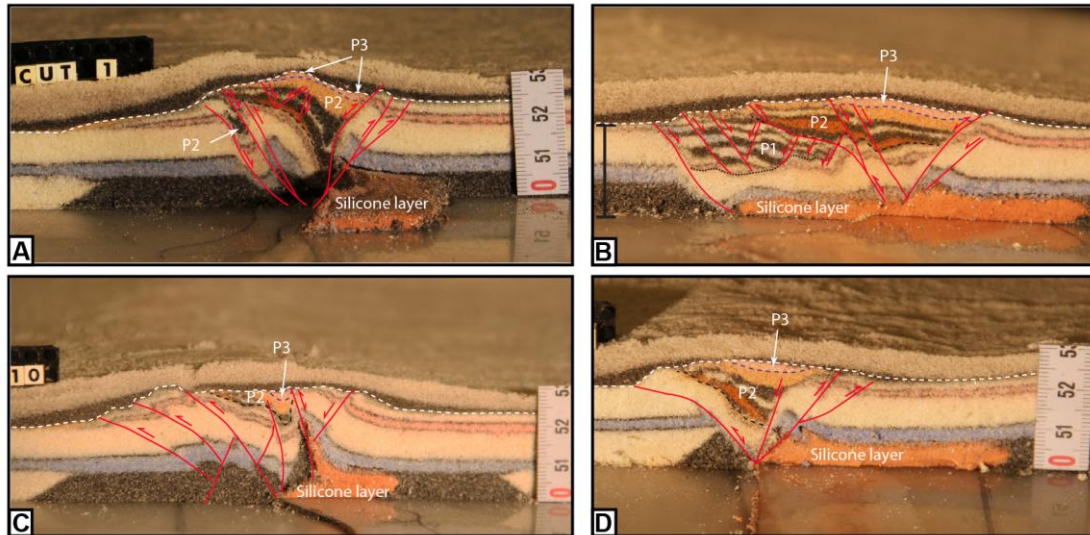
557 By a shear displacement of 0.55 cm additional curved splay faults were
558 initiated from the northern tip of the master fault of fault 3f; **Figure 7**), delineating
559 the northern margin of a rhombohedral pull-apart-basin (Mann et al., 1983; Mann,
560 2007; Christie-Blick & Biddle, 1985) and with a geometry that was
561 indistinguishable from pull-apart basins or rhomb grabens affiliated with
562 unbridged *en échelon* fault arrays (Crowell, 1974 a,b; Aydin & Nur, 1993).
563 Although sand was filled into the subsiding basins to minimize the graben relief



564
565 **Figure 8:** PSE-1 anticline-syncline pairs in segment 1 of experiment BarMar6 in
566 an oblique view (see **Figure 4** for position of Segment 1). PSE-1 folds (indicated
567 by relief defined by blue and yellow markers) were constrained to the central fault
568 zone (defined by Y-shear and its splay faults) and extended only 3-4 cm beyond it.
569 PSE-2 structures (incipient push-ups and positive flower structures) were
570 delineated by shear faults (black lines) and completely cannibalized PSE-1
571 structures by continued shear. Yellow and blue reference lines illustrate the
572 rotation of the fold axial trace caused by dextral shear. Already pre-shear distance
573 between the markers (blue and yellow lines) was 5cm. Black arrow indicates
574 shear direction.
575

576 and to prevent gravitational collapse, the sub-basins that were initiated in the
577 shear-stage were affected by internal cross-faults, and the initial basin units
578 remained the deepest so that the buried internal basin topography maintained a
579 high relief with several apparent depo-centers separated by intra-basinal
580 platforms. Systems of linked shear faults and PSE-structures became established
581 in the central part with neutral shear that separate the releasing and restraining
582 bends and development similarly to that seen for segment 3 (see below), but these
583 structures were soon destroyed by the interaction between the northern and
584 southern tips of the extensional and contractional shear duplexes (**Figure 10**).
585 The first structure to develop in the regime of the restraining bend (segment 2;
586 was a top-to-the-southwest (antithetic) thrust fault at an angle of 145° with the
587 regional trend of the basement border as defined by segments 1 and 3 (Fault 6). It
588 became visible by 0.5 cm of displacement. The northern part of segment 2 became,
589 however, dominated by a synthetic contractional top-to-the-northeast fault that
590 was initiated by 0.85 cm of shear (Fault 7; **Figures 5 and 6**). Thus, faults 6 and 7
591 delineated a growing half-crescent-shaped 5-7-cm wide push-up structure (Aydin
592 & Nur, 1982; Mann et al., 1983) south of the restraining bend (**Figure 9**; *PSE-4-*
593 *structures*). By continued shear these structures got the character of an antiformal
594 stack.

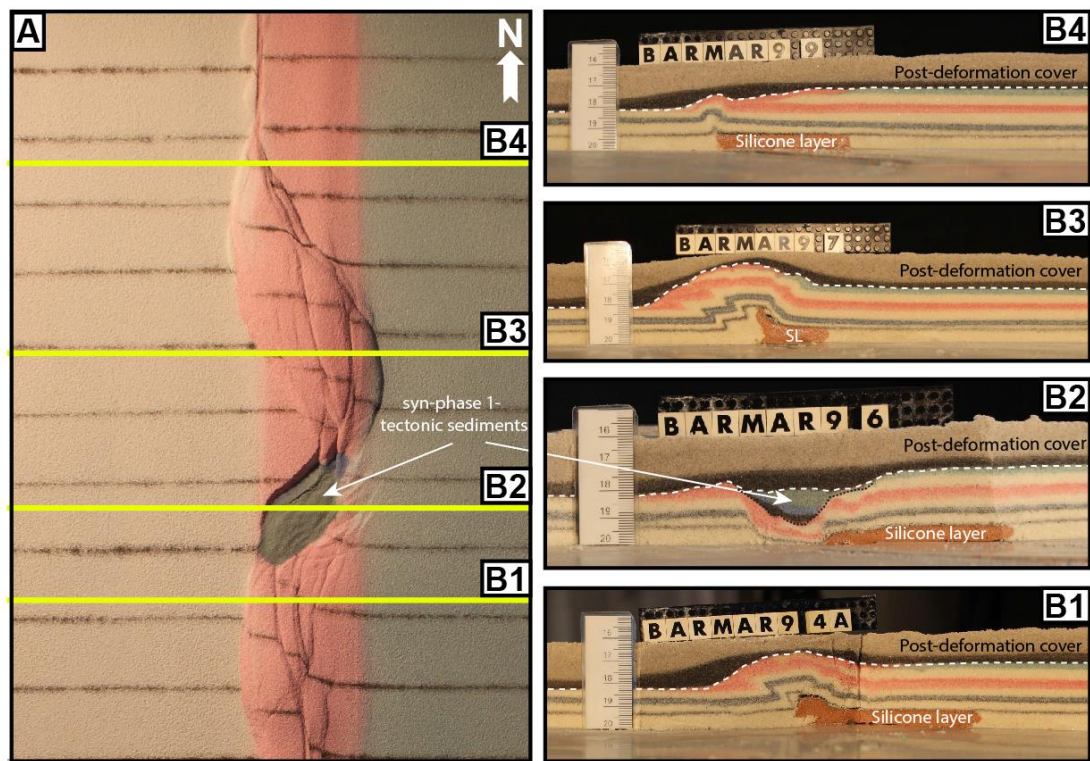
595 *Segment 3* defined a straight strand of neutral shear. Its development in the
596 BarMar-experiments followed strictly that known from numerous published
597 experiments (e.g. Tchalenko, 1970; Wilcox et al., 1973; Harding, 1974; Harding &
598 Lowell, 1979; Naylor et al., 1986; Sylvester, 1988; Richard et al., 1991; Woodcock
599 & Schubert, 1994; Dauteuil & Mart, 1998; Mann, 2007; Casas et al., 2001; Dooley
600 & Schreurs, 2012). A train of Riedel-shears, occupying the full length of the
601 segment, appeared simultaneously on the surface after a shear displacement of
602 0.5 cm, occupying a restricted zone with a width of 2-3 cm. The Riedel-shears
603 dominated the continued structural development of Segment 3. Riedel'-shears
604 were absent throughout the experiments, as should be expected for a sand-
605 dominated sequence (Dooley & Schreurs, 2012). P-shears developed by continued
606 shear, creating linked rhombic structures delineated by the Riedel- and P-shears
607 generating positive structural elements with NW-SE- and NNE-SSE-striking axes
608 (see also Morgenstern & Tchalenko, 1967), soon coalescing to form Y-shears.



609

610 **Figure 9:** Cross-sections through PSE-2-related structures. PSE-structures are
 611 marked with P and PSE-number as described in text (see also Table 1). **A)** Folded
 612 core of incipient push-up/positive flower structure in segment 1, experiment
 613 BarMar6. The fold structure is completely enveloped of shear faults that have a
 614 twisted along-strike geometry. Note that the eastern margin of the structure
 615 developed into a negative structure at a late stage in the development (filled by
 616 black-pink sand sequence) and that the silicone putty sequence (basal pink
 617 sequence) was entirely isolated in the footwall. **B)** Similar structure type in
 618 experiment BarMar8. However, the basal silicone putty layer here bridged the
 619 basal high-strain zone so that folding occurred in the footwall as well as in the
 620 hanging. Folds propagated up-section into the sand layers (blue). The folds in
 621 upper (pink) layers are younger and were associated with the contractional stage
 622 (PSE-6-structures). **C)** Contraction associated with “crocodile structure” in the
 623 footwall of the main fault in segment 1, experiment BarMar8. Note disharmonic
 624 folding with contrasting fold geometries in hanging wall and footwall and at
 625 different stratigraphic levels in the footwall, indicating that shifting stress
 626 situation in time and space occurred in the experiment. **D)** Transitional fault
 627 strand between to more strongly sheared fault segments (experiment BarMar9).
 628

629 Transverse sections document that these structures were cored by push-up
 630 anticlines, positive half-flower structures and full-fledged positive flower
 631 structures in the advanced stages of shear (*PSE-4-structures*) (**Figures 5 and 6;**
 632 **See also Figure 10**). These were accompanied by the development of *en échelon*
 633 folds and flower structures as commonly reported from strike-slip faults in nature
 634 and in experiments. The width of the zone above the basal fault remained almost
 635 constant throughout the experiments, but was somewhat wider in experiments
 636 with thicker basal silicone polymer layers, similar to that commonly described
 637 from comparable experiments (e.g. Richard et al., 1991).
 638



639

640 **Figure 10: A)** Contrasting structural styles along the master fault system in
 641 segment 2 in map view and **(B)** cross sections of experiment BarMar9. SL denotes
 642 silicone layer, the stippled line the boundary between pre- and syn-deformation
 643 layers and the white dashed line the boundary with the post-deformation layers.
 644

645 **Deformation Phase 2: Extension**

646 The late Cretaceous-Palaeocene dextral shear was followed by pure extension that
 647 accompanied the opening along the Barents Shear Margin in the Oligocene. Our
 648 experiments focused on the effects of oblique extension, acknowledging that plate
 649 tectonic reconstructions of the North Atlantic suggest an extension angle of 315°
 650 (Gaina et al., 2009).

651 All strike-slip basins widened in the extensional stage and as one would
 652 expect, the basins generated in orthogonal extension became wider than those
 653 generated in oblique extension. In both cases, however, extension promoted
 654 enhanced relief that had been generated in the shear-stage. In the earliest
 655 extensional stage, the strike-slip basin in segment 2 dominated the basin
 656 configuration. By continued extension the linear segments and the minor pull-
 657 apart basins in segments 1 and 2 started to open and became interlinked,
 658 subsequently generating a linked basin system that runs parallel to the entire
 659 shear margin (**Figures 5F-G, 6F-G**). The basins had become completely

660 interlinked by an extension of 1.25 cm (marked by the vertical dark blue line in
661 **Figure 7**). The orthogonal extension-phase also reactivated and linked several
662 master faults that were established in deformation phase 1 (**Figures 5A and 6A**).
663 This became evident by an extension of 0.25 – 0.50 cm and included the southern
664 fault margin, the push-up and the splay faults defining the crestal collapse graben
665 (Faults 6, 11 and 12; **Figure 4**). Among the faults that remained inactive
666 throughout the extension phase were the antithetic contractional fault delineating
667 the push-ups in segment 2 (Fault 6; **Figure 4**). The Y-shear in Segment 3 was
668 reactivated as a straight, continuous extensional fault in phase 2. Total extension
669 in stage 2 was 5 cm.

670

671 **Deformation Phase 3: contraction**

672 In our experiments the extension stage was followed by oblique contraction
673 (parallel to the direction of extension as applied for each experiment). A part of
674 the early-stage contraction was accommodated along new faults. It was more
675 common, however, that faults that had been generated in the strike-slip and
676 extensional stages became reactivated and rotated, and the development of
677 isolated folds, which were commonly associated with inverted fault traces,
678 generating snake-head or harpoon-structures structures (Cooper et al., 1989;
679 Coward, 1994; Allmendinger, 1998; Yameda & McClay, 2004; Pace & Calamitra,
680 2014; *PSE-5-structures*). The dominant structures affiliated with the contractional
681 stage was still new folds with traces oriented orthogonal to the shortening
682 direction and sub-parallel to the preexisting master fault systems that defined the
683 margin and basin margins (**Figure 12**). Also, some deep fold sets that had been
684 generated during the strike-slip phase and seen as domal surface features became
685 reactivated, causing renewed growth of surface structures (see **Figure 10** and
686 explanation in figure caption). These folds were generally up-right cylindrical
687 buckle folds in the initial contractional and with very large trace length:
688 amplitude-ratio (*SPE-6-structures*). Some intra-basin folds, however, defined fold
689 arrays that crossed the basins in a diagonal fashion. Particularly the folds situated
690 along the basin margins developed into fault propagation-folds above low-angle
691 thrust planes. Such faults aligning the western basin margins could have an
692 antithetic attitude relative to the direction of contraction.

693 During the contractional phase the margin-parallel, linked basin system
694 started immediately to narrow and several fault strands became inverted. The
695 basin-closure was a continuous process until the end of the experiment by 3 cm of
696 contraction. The contraction was initiated as a proxy for an ESE-directed ridge-
697 push stage. The first effect of this deformation stage was heralded by uplift of the
698 margin of the established shear zone that had developed into a rift during
699 deformation stage 2. This was followed by the reactivation and inversion of some
700 master faults (e.g. fault a2; **Figure 4**) and thereafter by the development of a new
701 set of low-angle top-to-the-ESE contractional faults. These faults displayed a
702 sequential development (fault family 1; **Figure 7**) and were associated with
703 folding of the strata in the rift structure, probably reflecting foreland-directed in-
704 sequence thrusting (SPE-5 and PSE-6 fold populations).

705

706 **Discussion**

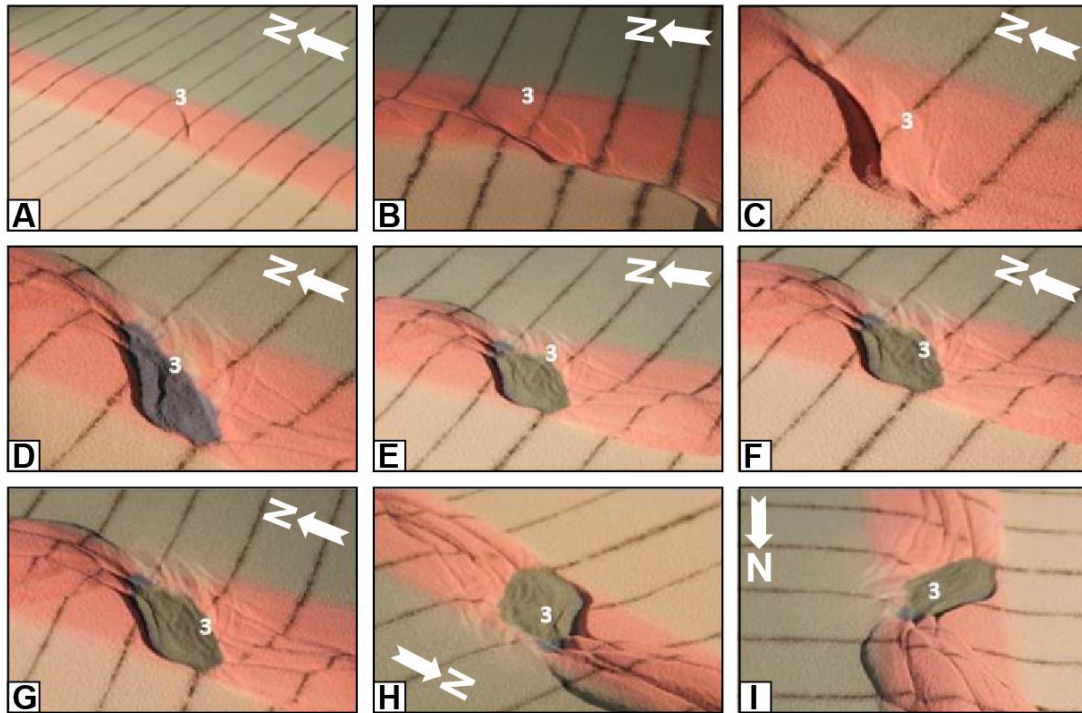
707 The break-up and subsequent opening of the Norwegian-Greenland Sea was a
708 multi-stage event (**Figure 13**) that imposed shifting stress configurations
709 overprinting the already geometrically complex Barents Shear Margin. Therefore,
710 scaled experiments were designed to illuminate its structural development. The
711 experiments utilized three main segments that correspond to the Senja Fracture
712 Zone (segment 1), the Vestbakken Volcanic Province (segment 2) and the
713 Hornsund Fault Zone (segment 3) respectively and three deformation phases
714 (dextral shear, oblique extension and contraction). Several structural families
715 (PSE 1-6) generated in the experiments correspond to structural features
716 observed in reflection seismic sections. In the following discussion we utilize
717 these two data sets in explaining the sequential development of each segment of
718 the shear margin.

719

720 **Structures of phase 1 (dextral shear)**

721 *Segment 1* (corresponding to the Senja Fracture Zone) was dominated by neutral
722 dextral shear, although jogs in the (pre-cut) fault provided minor sub-segments
723 with subordinate releasing and restraining bends.

724 PSE-1-folds seen in the incipient shear phase were confined to the area just above
725 the basal master fault (VD) and its immediate vicinity (see also experiments in

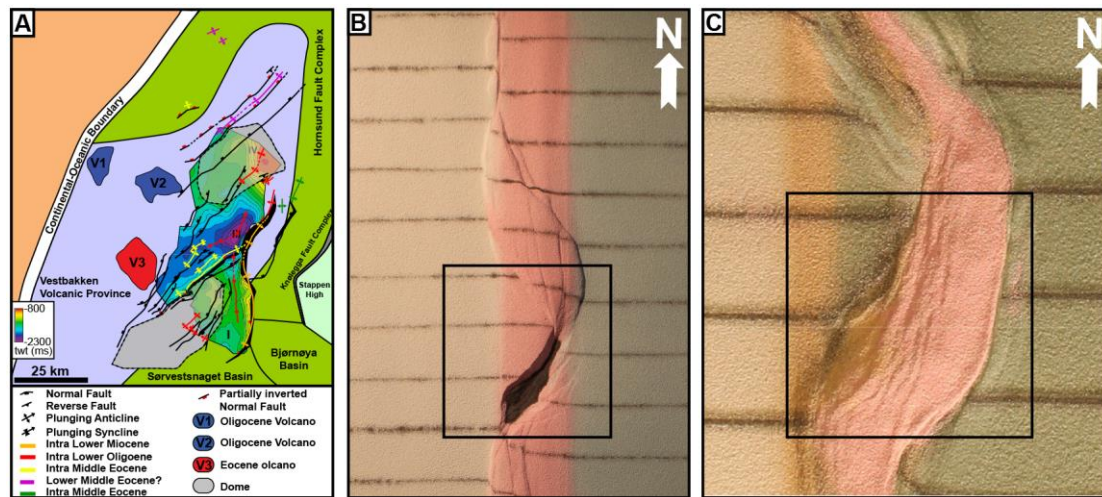


726

727 **Figure 11:** Nine stages in the development of the extensional shear duplex system
 728 above the releasing bend in experiment BarMar9. The master faults that
 729 developed at an incipient stage (e.g. Fault 3 that constrained the eastern margin
 730 of the extensional shear duplex, marked with "3" in the figure; see also **Figure 7**)
 731 remained stable and continued to be active throughout the experiment, but
 732 became overstepped by new faults in its footwall. These were reactivated as
 733 contraction faults at the later stages (stages H and I in this figure). The developing
 734 basement was stabilized by infilling of gray sand during this part of the experiment.
 735 Fault 3 remained broke through the basin infill also after the basin
 736 infill overstepped the original basin margin. The distance between the markers
 737 (dark lines) is 5cm. White arrow marks north-direction. Note that figures "H" and
 738 "I" (bottom right) is viewed from directions that differs from the other figures.
 739

740 series "e" and "f" of Mitra & Paul, 2011). Counterparts to PSE-1 structural
 741 population were not identified in the seismic data, although some isolated, local
 742 anticlinal features could be dismembered remnants of such. Because of their
 743 constriction to the near vicinity of the master fault it is reasonable that structures
 744 generated at an early stage of shear are vulnerable to cannibalization by younger
 745 structures with axes striking parallel to the main shear fault (Y-shears; SPE-2-
 746 structures). We therefore conclude that this structure population was destroyed
 747 during the later stages of shear and during the subsequent stages of extension and
 748 contraction.

749



750

751 **Figure 12:** PSE-5-folds generated during phase 3-inversion, experiment BarMar8.
 752 Note that fold axes mainly parallel the basin rims, but that they deviate from that
 753 in the central parts of the basins in some cases. The folds are best developed in
 754 segment 2, which accumulated extension in the combined shear and extension
 755 stages.

756

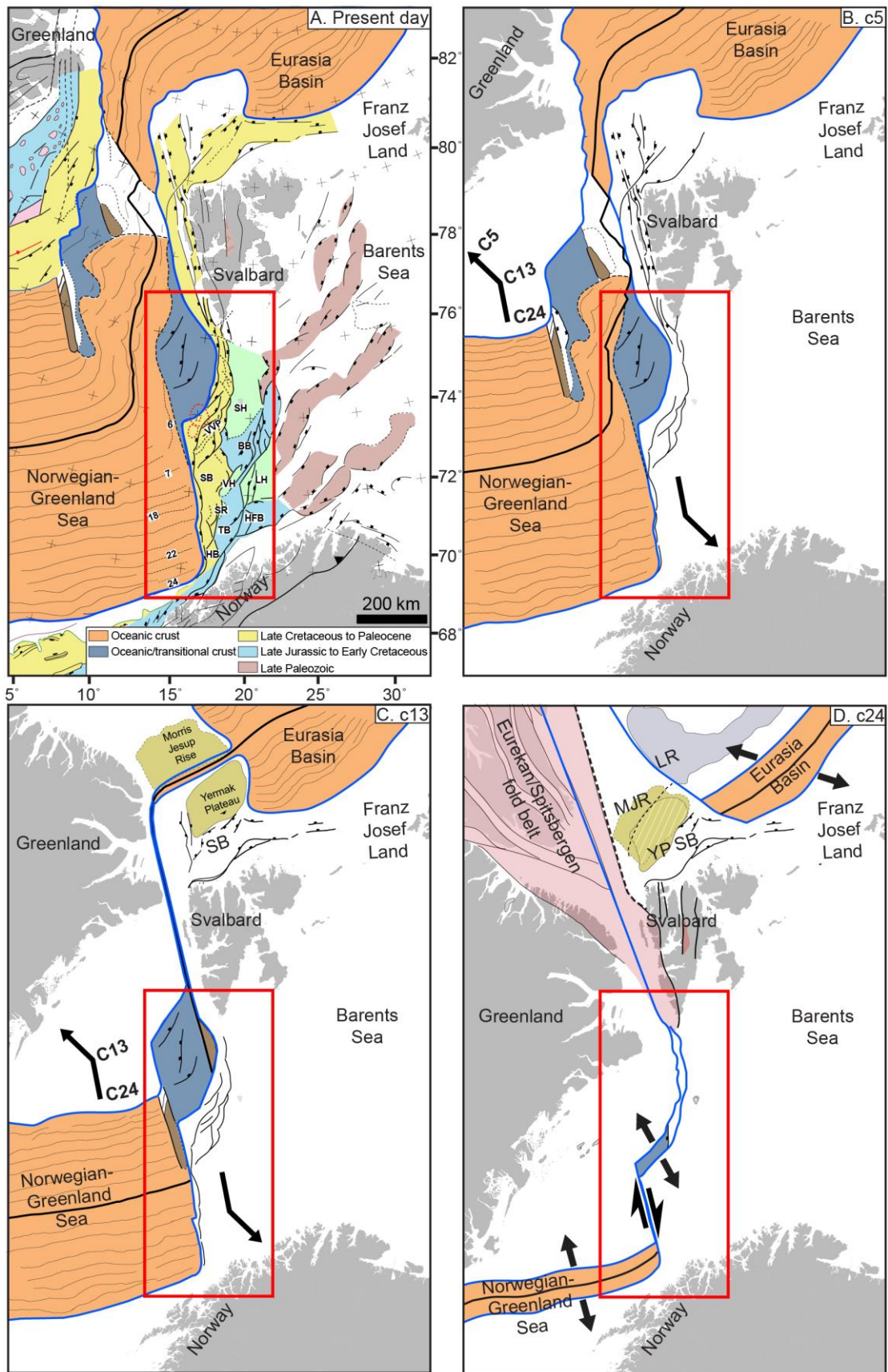
757 PSE-1-folds that developed at an incipient stage were immediately pursued by the
 758 development of two sets of NNE-SSW-striking normal faults with opposite throws
 759 in the releasing bend areas (e.g. fault 2 **Figure 4**). The two faults defined crescent-
 760 or spindle-shaped incipient extensional shear duplexes. These structures were
 761 stable during the remainder of the experiments and their master faults became
 762 reactivated during the extensional and contractional phases (see below). The
 763 most prominent of these structures corresponds to the position of the
 764 Sørvestsnaget Basin (**Figure 1B**).

765 *Segment 2*, which was controlled by a pre-cut crescent-shaped
 766 discontinuity in the experiments corresponds to the Vestbakken Volcanic
 767 Province and the southern extension of the Knølegga Fault Complex of the Barents
 768 Shear Margin (**Figures 1B and 4**). The Vestbakken Volcanic Province is
 769 dominated by interfering NNW-SSE- and NE-SW striking fold- and fault systems
 770 in its central part, whereas N-S-structures are more common along its eastern
 771 margin (**Figure 12A**) (Jebsen & Faleide, 1998; Giannenas, 2018). Intra-basinal
 772 highs and other internal configurations seen in the BarMar-experiments mainly
 773 reflect step-wise collapse of the intrinsic basin that generated rotational fault
 774 blocks, the crests of which separated local sediment accumulations. Such
 775 structures are common in strike-slip basins (e.g. Dooley & McClay, 1997; Dooley
 776 & Schreurs, 2012) and are consistent with the intra-basin depo-centers seen

777 within the Vestbakken Volcanic province and in the Sørvestsnaget Basin as well
778 (Knutsen & Larsen, 1997; Jebesen & Faleide, 1998; **Figure 13**). The crests of the
779 rotating fault blocks are termed PSE-3-structures above, and such eroded fault
780 block crests are defining the footwalls of major faults in the Vestbakken Volcanic
781 Province, providing space for sediment accumulation in the footwalls. The area
782 that was affected by the basin formation in the extensional shear duplex stage
783 seems to have remained the deepest part of the Vestbakken Volcanic Province,
784 whereas the part formed in basin widening by sequential footwall collapse created
785 a shallower sub-platform (*sensu* Gabrielsen, 1986) (**Figure 11**).

786 The Knølegga Fault Complex occupies a km-wide zone in segment 2. The
787 master fault strand is paralleled by faults with significant normal throws on its
788 hanging wall side and this belongs to the larger Knølegga Fault Complex (EBF;
789 Eastern Boundary Fault; Giannenas, 2018; **Figure 12A**). The EBF zone is a top-
790 west normal fault with maximum throw of nearly 2000 ms (3000 meters). It can
791 be followed along its strike for more than 60 km and seems to die out by horse-
792 tailing at its tip-points. The vicinity of the master faults of the Knølegga Fault
793 Complex locally display isolated elongate positive structures constrained by
794 steeply dipping faults. These structures sometimes display internal reflection
795 patterns that seem exotic in comparison to the surrounding sequences. Some of
796 these structures resemble positive flower structures or push-ups or define narrow
797 anticlines. They are found in both the footwall and hanging wall of the border
798 faults and strike parallel to those and the axes of these structures parallel the
799 master faults. The traces of such structures can be followed over shorter distances
800 than the master faults, and do not occur in the central parts of the Vestbakken
801 Volcanic Province. We suggest that the composite geometry of the Knølegga Fault
802 Complex is due to the development of PSE-2-structures within the realm of a pre-
803 existing normal fault zone.

804 Due to the right-stepping geometry during dextral shear in segment 2, the
805 southern and northern parts were in the releasing and restraining bend positions,
806 respectively (e.g. Christie-Blick & Biddle, 1985). Hence, the southern part of
807 segment 2 was subject to oblique extension, subsidence and basin formation while
808 the northern part was subject to oblique contraction, shortening and uplift. The



809

810 **Figure 13;** Main stages in opening of the North Atlantic. The figure builds on figure

811 5 in Faleide et al. (2008) and has been updated and redrawn.

812

813 southern segment expanded to the east and northeast by footwall collapse and
814 activation of rotating fault blocks that contributed to a basin floor topography that
815 affected the pattern of sediment accumulation (**Figure 9A,B**).

816 The positive structural elements that prevail in *segment 3* belong to the
817 PSE-2-structure population. The structures affiliated with segment 3 in the
818 BarMar-experiments are similar to those seen in the reflection seismic sections
819 along parts of the Spitsbergen and the Senja shear margins (Myhre, et al. 1982)
820 and elsewhere (Cloos, 1928; Riedel, 1929; Tchalenko, 1970; Wilcox et al., 1973).
821 In the experiments *en echelon* folds (corresponding to PSE-1-structures) first
822 became visible, to be succeeded by the development of Riedel- and P-shears (R'-
823 shears were subdued as expected for sand-dominated sequences (Dooley &
824 Schreurs, 2012). Continued shear followed by collapse and interaction between
825 Riedel and P-shears and the subsequent development of Y-shears initiated push-
826 up- and flower-structure with N-S-axes (PSE-2) structures that were expressed as
827 non-cylindrical (double-plunging) anticlines on the surface (e.g. Tchalenko, 1970;
828 Naylor et al., 1986). Structures similar to the PSE-2-structures that were initiated
829 in the present experiments are common in scaled experiments with mechanically
830 stratified sequences where viscous basal strata are covered by sand (e.g. Richard
831 et al., 1991; Dauteuil & Mart, 1998).

832

833 **Structures of phase 2 (extension)**

834 It is expected that (regional) basin and (local) fault block subsidence became
835 accelerated during phase 2 (extension), and more so in the orthogonal extension
836 experiments (BarMar 6) than in the experiments with oblique extension (BarMar
837 8). However, due to stabilization of basins by infilling of sand, this was not
838 documented in the final photographs. The widening occurred mainly by fault-
839 controlled collapse of the footwalls, and dominantly along the master faults that
840 correspond to the Knølegga Fault Complex, but also new intra-basin cross-faults
841 that were initiated in the shear stage (see above) became reactivated, contributing
842 to the complexity of the basin topography. It is not likely that a stage was reached
843 where all (pull-apart) basin units along the margin became fully linked, although
844 sedimentary communication along the margin may have become established.

845 During the oblique extension stage segment 1 of experiments BarMar7-9
846 the basin subsidence was focused in the minor pull-apart basins, which soon
847 became linked along the regional N-S-striking basin axis. Remains of several such
848 basin centers, of which the Sørvestsnaget Basin (Knutsen & Larsen, 1997;
849 Kristiansen et al., 2017) is the largest, are preserved and found in seismic data
850 (**Figure 1B**). During the experiments a continuous basin system was developed in
851 the hanging wall side of the master fault. It is, however, not likely that linking of
852 shear basins occurred prior to the opening stage along the Barents Shear Margin.

853

854 **Structures of phase 3 (contraction)**

855 The contraction phase (phase 3) reactivated both normal and shear faults in the
856 master fault zone also causing folding in the hanging wall. Simultaneously rotation
857 of (intra-basinal) fault blocks and steepening of pre-existing faults occurred. New
858 fold populations (PSE-5-folds) with axial traces parallel to the basin axis and the
859 master faults characterized the inversion stage. Remnants of such folds are locally
860 preserved in the thickest sedimentary sequences affiliated with the Senja Shear
861 Margin.

862 Fold systems with fold axes paralleling the basin margins as seen in the
863 experiments are also common in the Vestbakken Volcanic Province. Although
864 shortening occurred inside individual reactivated fault blocks by large wavelength
865 bulging of the entire sedimentary sequence also trains of folds with larger
866 amplitude and shorter wavelength were developed at this stage (**Figure 12B,C**).
867 Thus, the tectonic inversion was focused along the N-S-striking basin margins but
868 also occurred along some pre-existing NE-SW-striking faults and in the central
869 parts of the basin.

870 During phase 3 the restraining bend configuration in the northern part of
871 segment 2 was characterized by increasing contraction across strike-slip fault
872 strands that splayed out to the northwest from the central part of segment 2 in an
873 early stage of dextral shear. This deformation was terminated by the end of phase
874 1 by stacking of oblique contraction faults (PSE-5 and PSE-6-structures), defining
875 an antiformal stack-like structure. This type of deformation falls outside the
876 mapped area, but to the north this type of oblique shortening during the Eocene

877 (phase 1) was accommodated by regional-scale strain partitioning (Leever et al.,
878 2011a,b).

879 Also, the Vestbakken Volcanic Province is characterized by extensive
880 regional shortening. Onset of this event of inversion/contraction is dated to early
881 Miocene (Jebsen & Faleide, 1998, Giannenas, 2018) and this deformation included
882 two main structural fold styles. The first includes upright to steeply inclined closed to
883 open anticlines that are typically present in the hanging wall of master faults. These
884 folds typically have wavelengths in the order of 2.5 to 4.5 kilometers, and amplitudes
885 of several hundred meters. Most commonly they appear with head-on snakehead-
886 structures and are interpreted as buckle folds, albeit a component of shear may occur in
887 the areas of the most intense deformation. The second style includes gentle to open
888 anticline-syncline pairs with upright or steep to inclined axial planes with wavelengths
889 in the order of 5 to 7 kilometers and amplitudes of several tens of meters to several
890 hundred meters. We associate those with the PSE-4-type structures as defined in the
891 BarMar-experiments. These folds are situated in positions where sedimentary
892 sequences have been pushed against buttresses provided by master faults along the
893 basin margins. The PSE-6 folds developed as fold trains in the interior basins, where
894 buttressing against larger fault walls was uncommon. Also, this pattern fits well with
895 the development and geometry seen in the BarMar-experiments, where folding started
896 in the central parts of the closing basins before folding of the marginal parts of the
897 basin. In the closing stage the folding and inversion of master faults remained focused
898 along the basin margins.

899 The experiments clearly demonstrated that contraction by buckle folding
900 was the main shortening mechanism of the margin-parallel basin system
901 generated in phase 2 (orthogonal or oblique extension) in all segments. In the
902 Vestbakken Volcanic Province segments of the Knølegga Fault Complex, the EBF
903 and the major intra-basinal faults contain clear evidence for tectonic inversion,
904 whereas this is less pronounced in others. The hanging wall of the EBF is partly
905 affected by fish-hook-type inversion anticlines (Ramsey & Huber, 1987; Griera et
906 al., 2018) (**Figure 2D,E**), or isolated hanging wall anticlines or pairs or trains of
907 synclines and anticlines (e.g.; Roberts, 1989; Coward et al., 1991; Cartwright,
908 1989; Mitra, 1993; Uliana et al., 1995; Beauchamp et al. 1996; Gabrielsen et al.
909 1997; Henk & Nemcok 2008), the fold style and associated faults probably being

910 influenced by the orientation and steepness of the pre-inversion fault (Williams et
911 al., 1989; Cooper et al., 1989; Cooper & Warren, 2010). Some structures of this
912 type can still be followed for many kilometers having consistent geometry and
913 attitude. These structures have not been much modified by reactivation and are
914 invariably found in the proximal parts footwalls of master faults, suggesting that
915 these are inversion structures. They correlate to PSE-type 5-structures in the
916 experiments that developed in areas of focused contraction along pre-existing
917 fault scarps during Oligocene inversion.

918 Trains of folds with smaller amplitudes and higher frequency are
919 sometimes found in fault blocks in the central part of the Vestbakken Volcanic
920 Province (**Figure 12A**). Although these structures are not dateable by seismic
921 stratigraphical methods (on-lap configurations etc.) we regard these fold strains
922 to be correlatable with the tight folds generated in the inversion stage in the
923 experiments (PSE-6-structures) and that they are contemporaneous with the PSE-
924 5-structures.

925 Segment 1 in the experiments, that corresponds to the Senja Shear Margin
926 , displays a structural pattern that is a hybrid between segments 1 and 2: It
927 contains incipient structural elements that were developed in full in segments 2
928 and 3, segment 2 being dominated by releasing and restraining bend
929 configurations and segment 3 dominated by neutral shear. Due to internal
930 configurations, the three segments were affected to secondary (oblique) opening
931 and contraction in various fashions. Understanding these differences was much
932 promoted by the comparison of seismic and model data.

933

934 **Some considerations about multiphase deformation in shear margins**

935 The Barents Shear Margin is a challenging target for structural analysis both
936 because it represents a geometrically complex structural system with a multistage
937 history, but also because high-quality (3D) reflection seismic data are limited and
938 many structures and sedimentary systems generated in the earlier tectono-
939 thermal stages have been overprinted and obliterated by younger events. This
940 makes analogue experiments very useful in the analysis, since they offer a
941 template for what kind of structural elements can be expected. By constraining the
942 experimental model according to the outline of the margin geometry and imposing

943 a dynamic stress model in harmony according to the state-of-the-art knowledge
944 about the regional tectono-sedimentological development, we were able to
945 interpret the observations done in reflection seismic data in a new light.

946 Continental margins are commonly segmented containing primary or
947 secondary transform elements, and pure strike-slip transforms are relatively rare
948 (e.g. Nemcok et al. 2016). Such margins, however, invariably become affected by
949 extension following break-up and sometimes contraction due to ridge-push or far-
950 field stress perhaps related to plate reorganization. The complexity of shear
951 margins has ignited several conceptual discussions. One such discussion concerns
952 the presence of zones of weakness prior to break-up (e.g. Sibuet & Mascle 1978;
953 Taylor et al, 2009; Gibson et al. 2013; Basile 2015). In the case of the Barents Shear
954 Margin the de Geer zone provides such a pre-existing zone of weakness, and this
955 premise was acknowledged when the scaled model was established. The
956 relevance of our model is therefore constrained to cases where a crustal-scale
957 zone of weakness existed before break-up. Furthermore, in cases with pre-
958 existing zones of weakness, our model demonstrates that the incipient
959 architecture of the margin is important indeed and the detailed geometry and
960 width of the pre-existing weak zone must be mapped and included in the model.

961

962 **Summary and conclusions**

963 Our observations confirmed that the main segments of the Barents Shear Margin,
964 albeit undergoing the same regional stress regime, display contrasting structural
965 configurations. The deformation in segment 2 in the BarMar-experiments, was
966 determined by releasing and restraining bends in the southern and northern
967 parts, respectively. Thus, the southern part, corresponding to the Vestbakken
968 Volcanic Province, was dominated by the development of a regional-scale
969 extensional shear duplex as defined by Woodcock & Fischer (1983) and Twiss &
970 Moores (2007). By continued shear the basin developed into a full-fledged pull-
971 apart basin or rhomb graben (Crowell, 1974; Aydin & Nur, 1982) in which rotating
972 fault blocks were trapped. The pull-apart-basin became the nucleus for greater
973 basin systems to develop in the following phase of extension also providing the
974 space for folds to develop in the contractional phase.

975 We conclude that fault- and fold systems found in the realm of the
976 Vestbakken Volcanic Province are in accordance with a three-stage development
977 that includes dextral shear followed by oblique extension and contraction
978 (315/135°) along a shear margin with composite geometry. Folds with NE-SW-
979 trending fold axes are dominant in wider area of the Vestbakken Volcanic Province
980 and are dominated by folds in the hanging walls of (older) normal faults,
981 sometimes characterized by narrow, snake-head- or harpoon-type structures that
982 are typical for tectonic inversion (Cooper et al., 1989; Coward, 1994;
983 Allmendinger, 1998; Yameda & McClay, 2004; Pace & Calamitra, 2014).

984 Comparing seismic mapping and analogue experiments it is evident that a
985 main challenge in analyzing the structural pattern in shear margins of complex
986 geometry and multiple reactivation is the low potential for preservation of
987 structures that were generated in the earliest stages of the development.

988
989
990
991
992
993
994
995
996
997
998
999
1000
1001
1002
1003
1004
1005
1006
1007

1008 **Author contribution**

1009 R.H.Gabrielsen: Contributions to outline, design and performance of experiments.

1010 First writing and revisions of manuscript. First drafts of figures.

1011 P.A.Giannenas: Seismic interpretation in the Vestbakken Volcanic Province.

1012 Identification and description of fold families.

1013 Suggestion:

1014 D.Sokoutis: Main responsibility for set-up, performance and handling of
1015 experiments. Revisions of manuscript.

1016 E.Willigshofer: Performance and handling of experiments. Revisions of
1017 manuscript. Design and revisions of figure material.

1018 M. Hassaan: Background seismic interpretation. Discussions and revisions of
1019 manuscript. Design and revisions of figure material.

1020 J.I.Faleide: Regional interpretations and design of experiments. Participation in
1021 performance and interpretations of experiments. Revisions of manuscript, design
1022 and revisions of figure material.

1023

1024 **Acknowledgements**

1025 The work was supported by ARCEX (Research Centre for Arctic Petroleum
1026 Exploration), which was funded by the Research Council of Norway (grant number
1027 228107) together with 10 academic and six industry (Equinor, Vår Energi, Aker
1028 BP, Lundin Energy Norway, OMV and Wintershall Dea) partners. Muhammad
1029 Hassaan was funded by the Suprabasins project (Research Council of Norway
1030 grant no. 295208). We thank to Schlumberger for providing us with academic
1031 licenses for Petrel software to do seismic interpretation. Two anonymous
1032 reviewers and the editors of this special volume provided comments, suggestions
1033 and advice that enhanced the clarity and scientific quality of the paper.

1034

1035

1036

1037

1038

1039

1040

1041

1042

1043

1044 **References**

1045

1046 Allemand P. and Brun J.P.: Width of continental rifts and rheological layering of the
1047 lithosphere. *Tectonophysics*, 188, 63-69, 1991.

1048 Allmendinger,R.W.: : Inverse and forward numerical modeling of threeshear fault-
1049 propagation folds, *Tectonics*, 17(4), 640-656, 1998.

1050 Auzemery, A., E. Willingshofer, D. Sokoutis, J.P. Brun and Cloetingh S.A.P.L.,:
1051 Passive margin inversion controlled by stability of the mantle lithosphere,
1052 *Tectonophysics*, 817, 229042, 1-17, <https://doi.org/10.1016/j.tecto.2021.229042>, 2021.

1053 Aydin,A. and Nur,A.:1982: Evolution of pull-apart basins and their scale independence.
1054 *Tectonics*, 1, 91-105, 1982.

1055

1056 Ballard J-F., Brun J-P and Van Ven Driessche J.: Propagation des chevauchements au-
1057 dessus des zones de décollement: modèles expérimentaux. *Comptes Rendus de*
1058 *l'Académie des Sciences, Paris*, 11, 305, 1249-1253, 1987.

1059

1060 Basile, C.: Transform continental margins – Part 1: Concepts and models.
1061 *Tectonophysics*, 661, pp.1-10. doi: 10.1016/j.tecto.2015.08.034, 2015.

1062

1063 Basile,C. and Brun,J.-P.: Transtensional faulting patterns ranging from pull-apart
1064 basins to transform continental margins: an experimental investigation, *Journal of*
1065 *Structural Geology*, 21,23-37, 1997.

1066

1067 Beauchamp,W., Barazangi,M., Demnati,A. and El Alji,M.: Intracontinental rifting and
1068 inversion: Missouri Basin and Atlas Mountains, Morocco. *American Association of*
1069 *Petroleum Geologists Bulletin*, 80(9), 1455-1482, 1996.

1070

1071 Bergh,S.G., Braathen,A. and Andresen,A.: Interaction of basement-involved and thin-
1072 skinned tectonism in the Tertiary fold-and-thrust belt of Central Spitsbergen, Svalbard.
1073 *American Association of Petroleum Geologists Bulletin*, 81(4), 637-661,1997.

1074

1075 Bergh,S.G. and Grogan,P.: Tertiary structure of the Sørkapp-Hornsund Region, South
1076 Spitsbergen, and implications for the offshore southern extension of the fold-thrust-
1077 belt. *Norwegian Journal of Geology*, 83, 43-60, 2003.

1078

1079 Biddle, K.T. and Christie-Blick, N., (eds.): *Strike-Slip Deformation, Basin Formation,*
1080 *and Sedimentation: Society of Economic Paleontologists and Mineralogists Special*
1081 *Publication*, 37, 386pp, 1985a.

1082

1083 Biddle, K.T. and Christie-Blick, N.: Glossary — Strike-slip deformation, basin
1084 formation, and sedimentation, in: Biddle, K.T., and Christie-Blick, N. (eds.): *Strike-*
1085 *Slip Deformation, Basin Formation, and Sedimentation: Society of Economic*
1086 *Paleontologists and Mineralogists Special Publication*, 37, 375-386, 1985b

1087

1088 Blaich,O.A., Tsikalas,F. and Faleide,J.I.: New insights into the tectono-stratigraphic
1089 evolution of the southern Stappen High and the transition to Bjørnøya Basin, SW
1090 Barents Sea, *Marine and Petroleum Geology*, 85, 89-105, doi:
1091 10.1016/j.marpetgeo.2017.04.015, 2017.

- 1092
1093 Breivik,A.J., Faleide,J.I. and Gudlaugsson,S.T.: Southwestern Barents Sea margin: late
1094 Mesozoic sedimentary basins and crustal extension, *Tectonophysics*, 293, 21-44, 1998.
1095
1096 Breivik,A.J., Mjelde,R., Grogan,P., Shinamura,H., Murai,Y. and Nishimura,Y.: Crustal
1097 structure and transform margin development south of Svalbard based on ocean bottom
1098 seismometer data. *Tectonophysics*, 369, 37-70 2003.
- 1099 Brekke, H.: The tectonic evolution of the Norwegian Sea continen- tal margin with
1100 emphasis on the Vøring and Møre basins: Geological Society, London, Special
1101 Publication, 136, 327–378, 2000.
- 1102 Brekke, H. and Riis, F.: Mesozoic tectonics and basin evolution of the Norwegian Shelf
1103 between 60°N and 72°N. *Norsk Geologisk Tidsskrift*, 67, 295-322, 1987.
1104
1105 Burchfiel, B.C. and Stewart,J.H.: "Pull-apart" origin of the central segment of Death
1106 Valley, California. *Geological Society of America Bulletin*, 77, 439-442, 1966.
1107
1108 Campbell,J.D.: *En échelon* folding, *Economical Geology*, 53(4), 448-472, 1958.
1109
1110 Cartwright,J.A.: The kinematics of inversion in the Danish Central Graben. in:
1111 M.A.Cooper & G.D.Williams (eds.): *Inversion Tectonics*. Geological Society of
1112 London Special Publication, 44, 153-175, 1989.
1113
1114 Casas, A.M., Gapals,D., Nalpas,T., Besnard,K. and Román-Berdiel,T.: Analogue
1115 models of transpressive systems, *Jornal of Structural Geology*, 23,733-743, 2001
1116
1117 Christie-Blick,N. and Biddle,K.T.: Deformation and basin formation along strike-slip
1118 faults. in: Biddle,K.T. & Christie-Blick,N. (eds.): *Strike-slip deformation, basin
1119 formation and sedimentation*. Society of Economic Mineralogists and Palaeontologists
1120 (Tulsa Oklahoma), Special Publication, 37, 1-34, 1985.
1121
1122 Cloos,H.: Experimenten zur inneren Tectonick, *Zentralblatt für Mineralogie, Geologie
1123 und Palaentologie*, 1928B, 609-621, 1928.
1124
1125 Cloos,H.: Experimental analysis of fracture patterns, *Geological Society of America
1126 Bulletin*, 66(3), 241-256, 1955.
1127
1128 Cooper,M. and Warren,M.J.: The geometric characteristics, genesis and petroleum
1129 significance of inversion structures, in Law,R.D., Butler,R.W.H., Holdsworth,R.E.,
1130 Krabbendam,M. & Strachan,R.A. (eds.): *Continental Tectonics and Mountain
1131 Building: The Lagacy of Peache and Horne*, Geological Society of London, Special
1132 Publication, 335, 827-846, 2010.
1133
1134 Cooper,M.A., Williams,G.D., de Graciansky,P.C., Murphy,R.W., Needham,T., de
1135 Paor,D., Stoneley,R., Todd,S.P., Turner,J.P. and Ziegler,P.A.: Inversion tectonics – a
1136 discussion. Geological Society, London, Special Publications, 44, 335-347, 1989.
1137
1138 Coward, M.: Inversion tectonics, in: Hancock,P.L. (ed.): *Continental Deformation*,
1139 Pergamon Press, 289-304, 1994.

1140
1141 Coward, M.P., Gillcrist, R. and Trudgill, B.: Extensional structures and their tectonic
1142 inversion in the Western Alps, *in*: A.M.Roberts, G.Yielding & B.Freeman (eds.): The
1143 Geometry of Normal Faults. Geological Society of London Special Publication, 56, 93-
1144 112 1991.
1145
1146 Crowell, J.C.: Displacement along the San Andreas Fault, California, Geological
1147 Society of America Special Papers, 71, 59pp, 1962.
1148
1149 Crowell, J.C.: Origin of late Cenozoic basins in southern California. in Dorr, R.H. and
1150 Shaver, R.H. (eds.): Modern and ancient geosynclinal sedimentation. SEPM Special
1151 Publication, 19, 292-303, 1974a
1152
1153 Crowell, J.C., 1974b: Implications of crustal stretching and shortening of coastal
1154 Ventura Basin, *in*: Howell,D.G. (ed.): Aspects of the geological history of the
1155 California continental Borderland, American Association of Petroleum Geologists,
1156 Pacific Section,Publication, 24, 365-382, 1974b
1157
1158 Cunningham, W.D. and Mann, P. (eds.): : Tectonics of Strike-Slip Restraining and
1159 Releasing Bends, Geological Society London Special Publication, 290, 482pp, 2007a.
1160
1161 Cunningham, W.D. and Mann, P.: Tectonics of Strike-Slip Restraining and Releasing
1162 Bends, *in*: Cunningham,W.D. & Mann,P. (eds.), 2007: Tectonics of Strike-Slip
1163 Restraining and Releasing Bends, Geological Society London Special Publication, 290,
1164 1-12, 2007b.
1165
1166 Dauteuil, O. and Mart, Y.: Analogue modeling of faulting pattern, ductile deformation,
1167 and vertical motion in strike-slip fault zones, Tectonics, 17(2), 303-310, 1998.
1168
1169 Del Ventisette, C., Montanari, D., Sani, F., Bonini, M. and Corti, G.: Reply to comment
1170 by J. Wickham on ‘‘Basin inversion and fault reactivation in laboratory
1171 experiments’’. Journal of Structural Geology 29, 1417–1418, 2007.
1172
1173 Dooley, T. and McClay, K.: Analog modeling of pull-apart basins, American
1174 Association of Petroleum Geologists Bulletin, 81(11), 1804-1826, 1997.
1175
1176 Dooley, T.P. and Schreurs, G.:Analogue modelling of intraplate strike-slip tectonics: A
1177 review and new experimental results, Tectonophysics, 574-575, 1-71, 2012
1178
1179 Doré, A.G. and Lundin, E.R.: Cenozoic compressional structures on the NE Atlantic
1180 margin: nature, origin and potential significance for hydrocarbon exploration.
1181 Petroleum Geosciences, 2, 299-311, 1996
1182
1183 Doré, A.G., Lundin, E.R., Gibbons, A., Sømme, T.O. and Tørudbakken, B.O.:
1184 Transform margins of the Arctic: a synthesis and re-evaluation *in*: Nemcok,M.,
1185 Rybár,S., Sinha,S.T., Hermeston,S.A. & Ledvényiová,L. (eds.): Transform Margins,:
1186 Development, Control and Petroleum Systems, Geological Society London, Special
1187 Publication, 431, 63-94, 2016.
1188

1189 Doré, A.G., Lundin, E.R., Jensen, L.N., Birkeland, Ø., Eliassen, P.E. and Fichler, C.:
1190 Principal tectonic events in the evolution of the northwest European Atlantic margin.
1191 In: A.J.Fleet & S.A.R.Boldy (eds.): Petroleum Geology of Northwest Europe:
1192 Proceedings of the Fifth Conference (Geological Society of London), 41-61, 1999.
1193

1194 Eidvin, T., Goll, R.M., Grogan, P., Smelror, M. and Ulleberg, K.: The Pleistocene to
1195 Middle Eocene stratigraphy and geological evolution of the western Barents Sea
1196 continental margin ta well site 731675-1 (Bjørnøya West area). Norsk Geologisk
1197 Tidsskrift, 78, 99-123 1988.
1198

1199 Eidvin, T., Jansen, E. and Riis,F.: Chronology of Tertiary fan deposits off the western
1200 Barents Sea: Implications for the uplift and erosion history of the Barents Shelf. Marine
1201 Geology, 112, 109-131, 1993.
1202

1203 Eldholm, O., Faleide, J.I. and Myhre, A.M.: Continent-ocean transition at the western
1204 Barents Sea/Svalbard continental margin. Geology, 15, 1118-1122, 1987.
1205

1206 Eldholm, O., Thiede, J., and Taylor, E.: Evolution of the Vøring volcanic margin, *in*:
1207 Eldholm, O., Thiede, J., and Taylor, E., (eds.): Proceedings of the Ocean Drilling
1208 Program, Scientific Results, 104: College Station (Ocean Drilling Program), TX, 1033–
1209 1065, 1989.
1210

1211 Eldholm, O., Tsikalas, F. and Faleide,J.I.: Continental margin off Norway 62-
1212 75°N:Paleogene tectono-magmatic segmentation and sedimentation. Geological
1213 Society of London Special Publication, 197, 39-68, 2002
1214

1215 Emmons, R.C.: Strike-slip rupture patterns in sand models, Tectonophysics, 7, 71-87,
1216 1969.
1217

1218 Faugère, E., Brun, J.-P. and Van Den Driessche, J.: Bassins asymétriques en
1219 extension pure et en détachements:Modèles expérimentaux, Bulletin Centre Recherche
1220 Exploration et Production Elf Aquitaine, 10(2), 13-21, 1986.
1221

1222 Faleide, J.I., Bjørlykke, K. and Gabrielsen, R.H.: Geology of the Norwegian Shelf. *in*:
1223 Bjørlykke,K.: Petroleum Geoscience: From Sedimentary Environments to Rock
1224 Physics 2nd Edition, Springer-Verlag, Berlin Heidelberg, Chapter 25, 603 -637, 2015.
1225

1226 Faleide, J.I., Myhre, A.M. and Eldholm, O.: Early Tertiary volcanism at the western
1227 Barents Sea margin. in: A.C.Morton & L.M.Parsons (eds.): Early Tertiary volcanism
1228 and the opening of the NE Atlantic.Geological Society of London Special Publication,
1229 39,135-146, 1988.
1230

1231 Faleide, J.I., Tsikalas, F., Breivik, A.J, Mjelde, R., Ritzmann, O., Engen, Ø., Wilson, J.
1232 and Eldholm, O.: Structure and evolution of the continental margin off Norway and the
1233 Barents Sea. Episodes, 31(1), 82-91, 2008.
1234

1235 Faleide, J.I., Vågnes, E. and Gudlaugsson, S.T.: Late Mesozoic - Cenozoic evolution
1236 of the south-western Barents Sea in a regional rift-shear tectonic setting. Marine and
1237 Petroleum Geology, 10, 186-214, 1993
1238

- 1239 Fichler, C. and Pastore, Z.: Petrology and crystalline crust in the southwestern Barents
1240 Sea inferred from geophysical data. *Norwegian Journal of Geology*, 102, 41pp,
1241 <https://dx.doi.org/10.17850/njg102-2-2>, 2022.
1242
- 1243 Freund, R.: The Hope Fault, a strike-slip fault in New Zealand, *New Zealand
1244 Geological Survey Bulletin*, 86, 1-49, 1971.
1245
- 1246 Gabrielsen, R.H.: Structural elements in graben systems and their influence on
1247 hydrocarbon trap types. in: A.M. Spencer (ed.): *Habitat of Hydrocarbons on the
1248 Norwegian Continental Shelf*. *Norw. Petrol. Soc. (Graham & Trotman)*, 55 – 60, 1986.
1249
- 1250 Gabrielsen, R.H., Færseth, R.B., Jensen, L.N., Kalheim, J.E. and Riis, F.: Structural
1251 elements of the Norwegian Continental Shelf. Part I: The Barents Sea Region.
1252 *Norwegian Petroleum Directorate, Bulletin*, 6, 33pp, 1990.
1253
- 1254 Gabrielsen, R.H., Grunnaleite, I. and Rasmussen, E.: Cretaceous and Tertiary inversion
1255 in the Bjørnøyrenna Fault Complex, south-western Barents Sea. *Marine and Petroleum
1256 Geology*, 142, 165-178, 1997.
1257
- 1258 Gac, S., Klitzke, P., Minakov, A., Faleide, J.I. and Scheck-Wenderoth, M.:
1259 Lithospheric strength and elastic thickness of the Barents Sea and Kara Sea region,
1260 *Tectonophysics*, 691, 120-132, doi: 10.106/j.tecto.2016.04.028, 2016.
1261
- 1262 Gaina, C., Gernigon, L. and Ball, P.: Palaeocene – Recent plate boundaries in the NE
1263 Atlantic and the formation of the Jan Mayen microcontinent. *Journal of the Geological
1264 Society, London*, 166(4), 601-616, 2009.
- 1265 Ganerød, M., Smethurst, M.A., Torsvik, T.H., Prestvik, T., Rouse, S., McKenna, C.,
1266 van Hinsbergen, D.J.J. and Hendriks, W.W.H.: The North Atlantic Igneous Province
1267 reconstructed and its relation to the Plume Generation Zone: the Antrim Lava Group
1268 revisited. *Geophysical Journal International*, 182, 183-202, doi: 10.1111/j.1365-
1269 246X.2010.04620.x, 2010.
- 1270 Giannenas, P.A.: The Structural Development of the Vestbakken Volcanic Province,
1271 Western Barents Sea. Relation between Faults and Folds, Unpublished Ms.Sci.thesis,
1272 University of Oslo, 89 pp., 2018
1273
- 1274 Gibson, G.M., Totterdell, J.M., White, N. Mitchell, C.H., Stacey, A.R., M. P. Morse,
1275 M.P. and A. Whitaker: Preexisting basement structures and its influence on
1276 continental rifting and fracture development along Australia's southern rifted margin,
1277 *Journal of the Geological Society of London*, 170, 365-377, 2013.
1278 .
1279
- 1280 Graymer, R.W., Langenheim, V.E., Simpson, R.W., Jachens, R.C. and Ponce, D.A.:
1281 Relative simple through-going fault planes at large-earthquake depth may be concealed
1282 by surface complexity of strike-slip faults, *in*: Cunningham, W.D. & Mann, P. (eds.):
1283 *Tectonics of Strike-Slip Restraining and Releasing Bends*, Geological Society London
1284 *Special Publication*, 290, 189-201, 2007.
1285

- 1286 Griera, A., Gomez Rivas, E. and Llorens, M.-G.: The influence of layer-interface
1287 geometry of single-layer folding. Geological Society of London Special Publication
1288 487, SP487:4, 2018.
- 1289
1290 Grogan, P., Østvedt-Ghazi, A.-M., Larssen, G.B., Fotland, B., Nyberg, K., Dahlgren,
1291 S. and Eidvin, T.: Structural elements and petroleum geology of the Norwegian sector
1292 of the northern Barents sea. *in*: Fleet, A.J. & Boldry, S.A.R. (eds.): Petroleum Geology
1293 of Northwest Europe: Proceedings of the 5th Conference, Geological Society of
1294 London, 247-259, 1999.
- 1295
1296 Groshong, R.H.: Half-graben structures: balanced models of extensional fault bend
1297 folds, Geological Society of America Bulletin, 101, 96-195, 1989
- 1298
1299 Gudlaugsson, S.T. and Faleide, J.I.: The continental margin between Spitsbergen &
1300 Bjørnøya, in: O.Eiken (ed.): Seismic Atlas of Western Svalbard, Norsk Polarinstitutt
1301 Meddelelser, 130, 11-13, 1994.
- 1302
1303 Gudlaugsson, S.T., Faleide, J.I., Johansen, S.E. and Breivik, A.J.: Late Palaeozoic
1304 structural development of the south-western Barents Sea. Marine and Petroleum
1305 Geology, 15, 73-102, 1998.
- 1306
1307 Hamblin, W.K.: Origin of "reverse drag" on the down-thrown side of normal faults,
1308 Geological Society of America Bulletin, 76, 1145-1164, 1965.
- 1309
1310 Hanisch, J.: The Cretaceous opening of the Northeast Atlantic. Tectonophysics, 101, 1-
1311 23, 1984.
- 1312
1313 Harding, T.P.: Petroleum traps associated with wrench faults. American Association of
1314 Petroleum Geologists Bulletin, 58, 1290-1304, 1974.
- 1315
1316 Harding, T.P. and Lowell, J.D.: Structural styles, their plate tectonic habitats, and
1317 hydrocarbon traps in petroleum provinces, American Association of Petroleum
1318 Geologists Bulletin, 63, 1016-1058, 1979.
- 1319
1320 Harland, W.B.: The tectonic evolution of the Arctic-North Atlantic Region, in:
1321 Taylor, J.H., Rutten, M.G., Hales, A.L., Shackelton, R.M., Nairn, A.E. & Harland, W.B.:
1322 Discussion, A Symposium on Continental Drift, Philosophical Transactions of the
1323 Royal Society of London, Series A, 258, 1088, 59-75, 1965.
- 1324
1325 Harland, W.B.: Contributions of Spitsbergen to understanding of tectonic evolution of
1326 North Atlantic Region, American Association of Petroleum Geologists, Memoir 12,
1327 817-851, 1969.
- 1328
1329 Harland, W.B.: Tectonic transpression in Caledonian Spitsbergen, Geological
1330 Magazine, 108, 27-42, 1971
- 1331
1332 Henk, A. and Nemcok, M.: Stress and fracture prediction in inverted half-graben
1333 structures. Journal of Structural Geology, 30(1), 81-97, 2008.

- 1334 Horni, J.Á., Hopper, J.R., Blischke, A., Geisler, W.H., Stewart, M., Mcdermott, K.,
1335 Judge, M., Erlendsson, Ö. and Ártíng, U.E.: Regional Distribution of Volcanism within
1336 the North Atlantic Igneous Province. The NE Atlantic Region: A Reappraisal of
1337 Crustal Structure, Tectonostratigraphy and Magmatic Evolution. Geological
1338 Society, London, Special Publications, 447, 105–125,
1339 <https://doi.org/10.1144/SP447.18>, 2017.
- 1340 Horsfield, W.T., 1977: An experimental approach to basement-controlled faulting.
1341 *Geologie en Mijbouw*, 56(4), 3634-370 1977.
1342
- 1343 Hubbert, M.K.: Theory of scale models as applied to the study of geologic
1344 structures, *Bulletin Geological Society of America*, 48, 1459-1520, 1937.
- 1345 Jebsen, C. and Faleide, J.I.: Tertiary rifting and magmatism at the western Barents Sea
1346 margin (Vestbakken volcanic province). III international conference on Arctic margins,
1347 ICAM III; abstracts; plenary lectures, talks and posters, 92, 1998.
- 1348 Khalil,S.M. and McClay,K.R.: 3D geometry and kinematic evolution of extensional
1349 fault-related folds, NW Red Sea, Egypt. in: Childs,C., Holdswort,R.E., Jackson,C.A.L.,
1350 Manzocchi,T., Walsh,J.J & Yielding,G. (eds.): *The Geometry and Growth of Normal*
1351 *Faults*, Geological Society, London, Special Publication 439,
1352 doi.org/10.1144/SP439.11, 2016.
1353
- 1354 Klinkmüller, M., Schreurs, G., Rosenau, M. and Kemnitz, H.: Properties of
1355 granular analogue model materials: a community wide survey. *Tectonophysics*
1356 684, 23–38. <http://dx.doi.org/10.1016/j.tecto.2016.01.017.feb.>, 2016.
1357
- 1358 Knutsen, S.-M. and Larsen,K.I.,: The late Mesozoic and Cenozoic evolution of the
1359 Sørvestsnaget Basin: A tectonostratigraphic mirror for regional events along the
1360 Southwestern Barents Sea Margin? *Marine and Petroleum Geology*, 14(1), 27-54,
1361 1997.
1362
- 1363 Kristensen, T.B., Rotevatn, A., Marvik, M., Henstra, G.A., Gawthorpe, R.L. and
1364 Ravnås, R.: Structural evolution of sheared basin margins: the role of strain
1365 partitioning. *Sørvestsnaget Basin, Norwegian Barents Sea, Basin Research*, (2017), 1-
1366 23, doi:10.1111/bre.12235, 2017.
1367
- 1368 Le Calvez, J-H. and Vendeville, : Experimental designs to mode along strike-slip fault
1369 interaction. *in*: Scellart, W.P. & Passcheir, C. (eds.). *Analogue Modeling of large-scale*
1370 *Tectonic Processes*, *Journal of Virtual Explorer*, 7, 7-23, 2002.
1371
- 1372 Leever, K.A., Gabrielsen, R.H., Sokoutis, D. and Willingshofer, E.: The effect of
1373 convergence angle on the kinematic evolution of strain partitioning in transpressional
1374 brittle wedges: insight from analog modeling and high resolution digital image analysis.
1375 *Tectonics*, 30, TC2013, 1-25, doi: 10.1029/2009TC002649, 2011a.
1376
- 1377 Leever, K.A., Gabrielsen, R.H., Faleide, J.I. and Braathen, A.: A transpressional origin
1378 for the West Spitsbergen Fold and Thrust Belt - insight from analog modeling.
1379 *Tectonics*, 30, TC2014, 1- 24, doi: 10.1029/2010TC002753, 2011b.
1380

- 1381 Libak, A., Mjelde, R., Keers, H., Faleide, J.I. and Murai, Y.: An integrated geophysical
1382 study of Vestbakken Volcanic Province, western Barents Sea continental margin, and
1383 adjacent oceanic crust, *Marine Geophysical Research*, 33(2), 187-207, 2012.
- 1384
1385 Lorenzo, J.M.: Sheared continental margins: an overview, *Geo-Marine Letters*, 17(1),
1386 1-3, 1997
- 1387 Lowell, J.D., 1972: Spitsbergen Tertiary orogenic belt and the Spitsbergen fracture
1388 zone, *Geol. Soc. Am. Bull.*, 83, 3091–3102, doi:10.1130/0016-
1389 7606(1972)83[3091:STOBAT]2.0.CO;2, 1972.
- 1390 Lundin, E.R. and Doré, A.G.: A tectonic model for the Norwegian passive margin with
1391 implications for the NE Atlantic.: Early Cretaceous to break-up. *Journal of the*
1392 *Geological Society London*, 154, 545-550, 1997.
- 1393
1394 Lundin, E.R., Doré, A.G., Rønning, K. and Kyrkjebø, R.: Repeated inversion in the
1395 Late Cretaceous-Cenozoic northern Vøring Basin, offshore Norway, *Petroleum*
1396 *Geoscience*, 19(4), 329-341, 2013.
- 1397
1398 Luth, S., Willingshofer, E., Sokoutis, D. and Cloetingh, S.: analogue modelling of
1399 continental collision: Influence of plate coupling on mantle lithosphere subduction,
1400 crustal deformation and surface topography, *Tectonophysics*, 4184, 87-102, doi:
1401 10.1016/j.tecto2009.08.043, 2010.
- 1402 Maher, H. D., Jr., Bergh, S., Braathen, A. and Ohta, Y.: Svartfjella, Eidembukta, and
1403 Daudmannsodden lineament: Tertiary orogen-parallel motion in the crystalline
1404 hinterland of Spitsbergen's fold-thrust belt, *Tectonics*, 16(1), 88–106,
1405 doi:10.1029/96TC02616, 1997.
- 1406 Mandl, G., de Jong, L.N.J. and Maltha, A.: Shear zones in granular material. *Rock*
1407 *Mechanics*, 9, 95–144, 1977.
- 1408
1409 Manduit, T. and Dauteuil, O.: Small scale modeling of oceanic transform zones, *Journal*
1410 *of Geophysical Research*, 101(B9), 20195-20209, 1996.
- 1411
1412 Mann, P.: Global catalogue, classification and tectonic origins of restraining and
1413 releasing bends on active and ancient strike-slip fault systems. *in*: Cunningham, W.D.
1414 and Mann, P. (eds.), 2007: *Tectonics of Strike-Slip Restraining and Releasing Bends*,
1415 *Geological Society London Special Publication*, 290, 13-142, 2007.
- 1416
1417 Mann, P., Hempton, M.R., Bradley, D.C. and Burke, K.: Development of pull-apart
1418 basins. *Journal of Geology*, 91(5), 529-554, 1983.
- 1419
1420 Mascle, J. & Blarez, E.: Evidence for transform margin evolution from the Ivory Coast
1421 Ghana continental margin, *Nature*, 326, 378-381, 1987.
- 1422
1423 McClay, K.R., 1990: Extensional fault systems in sedimentary basins. A review of
1424 analogue model studies, *Marine and Petroleum Geology*, 7, 206-233, 1990.
- 1425
1426 Mitra, S.: Geometry and kinematic evolution of inversion structures. *American*

- 1427 Association of Petroleum Geologists Bulletin, 77, 1159-1191, 1993.
1428
- 1429 Mitra, S. and Paul, D.: Structural geology and evolution of releasing and restraining
1430 bends: Insights from laser-scanned experimental models, American Association of
1431 Petroleum Geologists Bulletin, 95(7), 1147-1180, 2011.
1432
- 1433 Morgenstern, N.R. and Tchalenko, J.S.: Microscopic structures in kaolin subjected to
1434 direct shear, Géotechnique, 17, 309-328, 1967.
1435
- 1436 Mosar, J., Torsvik, T.H. & the BAT Team: Opening of the Norwegian and Greenland
1437 Seas: Plate tectonics in mid Norway since the late Permian. in: E.Eide (ed.): BATLAS.
1438 Mid Norwegian plate reconstruction atlas with global and Atlantic perspectives.
1439 Geological Survey of Norway, 48-59, 2002.
1440
- 1441 Mouslopoulou, V., Nicol, A., Little, T.A. and Walsh, J.J.: Terminations of large-strike-
1442 slip faults: an alternative model from New Zealand, in: Cunningham, W.D. and Mann,
1443 P. (eds.): Tectonics of Strike-Slip Restraining and Releasing Bends, Geological Society
1444 London Special Publication, 290, 387- 415, 2007.
1445
- 1446 Mouslopoulou, V., Nicol, A., Walsh, J.J., Beetham, D. and Stagpoole, V.: Quaternary
1447 temporal stability of a regional strike-slip and rift fault interaction. Journal of Structural
1448 Geology, 30, 451-463, 2008.
1449
- 1450 Myhre, A.M. and Eldholm, O.: The western Svalbard margin (74-80°N). Marine and
1451 Petroleum Geology, 5, 134-156, 1988.
1452
- 1453 Myhre, A.M., Eldholm, O. and Sundvor, E.: The margin between Senja and Spitsbergen
1454 Fracture Zones: Implications from plate tectonics. Tectonophysics, 89, 33-50, 1982.
1455
- 1456 Naylor, M.A., Mandl, G and Sijpestijn, C.H.K.: Fault geometries in basement-induced
1457 wrench faulting under different initial stress states. Journal of Structural Geology, 8,
1458 737-752, 1986.
1459
- 1460 Nemcok, M., Rybár, S., Sinha, S.T., Hermeston, S.A. and Ledvényiová, L.: Transform
1461 margins: development, controls and petroleum systems – an introduction. in: Nemcok,
1462 M., Rybár, S., Sinha, S.T., Hermeston, S.A. and Ledvényiová, L. (eds.): Transform
1463 Margins,: Development, Control and Petroleum Systems, Geological Society London,
1464 Special Publication, 431, 1-38, 2016.
1465
- 1466 Odonne, F. and Vialon, P.: Analogue models of folds above a wrench fault,
1467 Tectonophysics, 99,31-46, 1983
1468
- 1469 Pace, P. and Calamita, F.: Push-up inversion structures v. fault-bend reactivation
1470 anticlines along oblique thrust ramps: examples from the Apennines fold-and-thrust-
1471 belt, Italy, Journal Geological Society London, 171, 227-238, 2014.
1472
- 1473 Pascal, C. and Gabrielsen, R.H.: Numerical modelling of Cenozoic stress patterns in
1474 the mid Norwegian Margin and the northern North Sea. Tectonics, 20(4), 585-599,
1475 2001.
1476

1477 Pascal, C., Roberts, D. and Gabrielsen, R.H.: Quantification of neotectonic stress
1478 orientations and magnitudes from field observations in Finnmark, northern Norway.
1479 Journal of Structural Geology, 27, 859-870, 2005.
1480
1481 Peacock, D.C.P., Nixon, C.W., Rotevatn, A., Sanderson, D.J. and Zuluaga, L.F.:
1482 Glossary of fault and other fracture networks, Journal of Structural Geology, 92,
1483 12-29, doi: 10.1016/j.jgs2016.09.008, 2016.
1484
1485 Perez-Garcia, C., Safranova, P.A., Mienert, J., Berndt, C. and Andreassen, K.:
1486 Extensional rise and fall of a salt diapir in the Sørvestsnaget Basin, SW Barents Sea.
1487 Marine and Petroleum Geology, 46, 129-134, 2013.
1488
1489 Planke, S., Alvestad, E. and Eldholm, O.: Seismic characteristics of
1490 basaltic extrusive and intrusive rocks: The Leading Edge, 18(3), 342-348. [https://doi-](https://doi-org.ezproxy.uio.no/10.1190/1.1438289)
1491 [org.ezproxy.uio.no/10.1190/1.1438289](https://doi-org.ezproxy.uio.no/10.1190/1.1438289), 1999.
1492
1493 Ramberg, H.: Gravity, deformation and the Earth's crust, Academic Press, New York,
1494 214pp, 1967.
1495
1496 Ramberg, H.: Gravity, deformation and the Earth's crust, 2nd edition. Academic Press,
1497 New York 452pp, 1981
1498
1499 Ramsay, J.G. and Huber, M.I., 1987: The techniques of modern structural geology. Vol.
1500 2: Folds and fractures. Academic Press, London, 309-700, 1987.
1501
1502 Reemst, P., Cloetingh, S. and Fanavoll, S.: Tectonostratigraphic modelling of Cenozoic
1503 uplift and erosion in the south-western Barents Sea. Marine and Petroleum Geology,
1504 11, 478-490, 1994.
1505
1506 Richard, P.D., Ballard, B., Colletta, B and Cobbold, P.R.: Naissance et evolution de
1507 failles au dessus d'un décrochement de socle: Modeléisation experimental et
1508 tomographie, C. R. Acad.Sci. Paris, 308,9, 2111-2118, 1989.
1509
1510 Richard, P.D. and Cobbold, P.R.: Structures et fleur positives et décrochements
1511 crustaux: mdélisation analogique et interpretation mécanique, C.R.Acad.Sci.Paris,
1512 308, 553-560, 1989.
1513
1514 Richard, P. and Krantz, R.W.: Experiments on fault reactivation in strike-slip mode,
1515 Tectonophysics, 188, 117-131, 1991.
1516
1517 Richard, P., Mocquet, B. and Cobbold, P.R., 1991: Experiments on simultaneous
1518 faulting and folding above a basement wrench fault, Tectonophysics, 188, 133-141.
1519 1991.
1520
1521 Riedel, W.: Zur Mechanik geologischer Brucherscheinungen. Centralblatt für
1522 Mineralogie, Geologie und Paläontologie, 1929B, 354-368, 1929.
1523
1524 Riis, F., Vollset, J. & Sand, M.: Tectonic development of the western margin of the
1525 Barents Sea and adjacent areas. in: M.T.Halbouty (ed.): Future petroleum provinces of
1526 the World. American Association of Petroleum Geologists Memoir, 40, 661-667, 1986.

- 1527
1528 Roberts, D.G., : Basin inversion in and around the British Isles, in: M.A.Cooper &
1529 G.D.Williams (eds.): Inversion Tectonics. Geological Society of London Special
1530 Publication, 44, 131-150, 1989.
1531
1532 Ryseth, A., Augustson, J.H., Charnock, M., Haugrud, O., Knutsen., S.-M-, Midbøe,
1533 P.S., Opsal, J.G. and Sundsbø,G.: Cenozoic stratigraphy and evolution of the
1534 Sørvestsnaget Basin, southwestern Barents Sea. Norwegian Journal of Geology, 83,
1535 107-130, 2003.
- 1536 Saunders, A.D., Fitton, J.G., Kerr, A.C., Norry, M.J., and Kent, R.W.: The North
1537 Atlantic Igneous Province: Geophysical Monograph 100, American Geophysical
1538 Union, 45–93, 1997.
- 1539 Scheurs, G.: Experiments on strike-slip faulting and block rotation, *Geology*, 22,567-
1540 570, 1990.
1541
1542 Schreurs, G.: Fault development and interaction in distributed strike-slip shear zones:
1543 an experimental approach. *in: Storti, F., Holdsworth, R.E. and Salvini, F. (eds):*
1544 *Intraplate Strike-slip Deformation Belts*, Geological Society of London Special
1545 Publication, 210, 35-82., 2003.
1546
1547 Schreurs, G., and Colletta, B.. Analogue modelling of faulting in zones of continental
1548 transpression and transtension. *in: Holdsworth, R.E., Strachan, R.A., Dewey, J.F.*
1549 *(eds.), Continental Transpressional and Transtensional Tectonics*, Geological
1550 Society of London Special Publication, London, 135, 59–79, 1998.
1551
1552 Schreurs, G. and Colletta, B.: Analogue modelling of continental transpression and
1553 transtension. *in: Scellart,W.P. & Passchier,C. (eds.): Analogue Modelling of Large-*
1554 *scale Tectonic Processes. Journal of the Virtual Explorer*, 7, 103-114, 2003.
1555
1556 Seiler, C., Fletcher, J.M., Quigley, M.C., Gleadow, A.J and Kohn, B.P.: Neogene
1557 structural evolution of the Sierra San Felipe, Baja California: evidence of proto-gulf
1558 transtension in the Gulf Extensional Province? *Tectonophysics*, 488(1), 87-109, 2010.
1559
1560 Sibuet, J.C. and Mascle ,J.: Plate kinematic implications of Atlantic equatorial
1561 fracture zone trends. *Journal of Geophysical Research*, 85, 3401-3421, 1978.
1562 Sims, D., Ferrill, D.A. and Stamatakos, J.A.: Role of a brittle décollement in the
1563 development of pull-apart basins: experimental results and natural examples. *Journal*
1564 *of Structural Geology*, 21, 533-554, 1999.
1565
1566 Sokoutis D.: Finite strain effects in experimental mullions. *Journal of Structural*
1567 *Geology*, 9, 233-249, 1987.
- 1568 Stearns, D.W., 1978: Faulting and forced folding in the Rocky Mountains Foreland,
1569 Geological Society of America Memoir, 151, 1-38, 1978
1570
1571 Sylvester, A.G. (ed); 1985: Wrench Fault Tectonics, Selected papers reprinted from the
1572 AAPG Bulletin and other geological journals, American Association of Petroleum
1573 Geologists Reprint Series 28,3 74pp, 1985.

- 1574
1575 Sylvester, A.G.: Strike-slip faults. Geological Society of America Bulletin, 100, 1666-
1576 1703, 1988.
1577
1578 Taylor,B., Goodlife,A. and Martinez,F.: Intiation of transform faults at rifted
1579 continental margins, Comtes Rendu Geosciences, 341, 428-438, 2009.
1580
1581 Talwani, M. & Eldholm, O.: Evolution of the Norwegian-Greenland Sea. Geological
1582 Society of America Bulletin, 88, 969-999, 1977.
1583
1584 Tchalenko, J.S: Similarities between shear zones of different magnitudes. Geological
1585 Society of America Bulletin, 81, 1625-1640,1970
- 1586 Tron, V. and Brun J-P.: Experiments on oblique rifting in brittle-ductile systems.
1587 Tectonophysics, 188(1/2), 71-84, 1991.
- 1588 Twiss, R.J. and Moores, E.M.: Structural Geology, 2nd Edition, W.H.Freeman & Co.,
1589 New York, 736pp, 2007.
1590
1591 Ueta, K., Tani ,K. and Kato,T.: Computerized X-ray tomography analysis of three-
1592 dimensional fault geometries in basement-induced wrench faulting, Engineering
1593 Geology, 56, 197-210, 2000
1594
1595 Uliana, M.A., Arteaga, M.E., Legarreta, L., Cerdan, J.J. and Peroni, G.O.: Inversion
1596 structures and hydrocarbon occurrence in Argentina. *in*: Buchanan,J.G. &
1597 Buchanan,P.G. (eds.): Basin Inversion, Geological Society London Special
1598 Publication, 88, 211-233, 1995
1599
1600 Vågnes,E.,1997: Uplift at thermo-mechanically coupled ocean-continent transforms:
1601 modeled at the Senja Fracture Zone, southwestern Barents Sea. Geo-Marine Letters,
1602 17, 100-109, 1997.
- 1603 Vågnes, E., Gabrielsen, R.H. and Haremo. P.: Late Cretaceous-Cenozoic intraplate
1604 contractional deformation at the Norwegian continental shelf: timing, magnitude and
1605 regional implications. Tectonophysics, 300, 29-46, 1998.
- 1606 Weijermars, R. and Schmeling, H.: Scaling of Newtonian and non-Newtonian fluid
1607 dynamics without inertia for quantitative modelling of rock flow due to gravity
1608 (including the concept of rheological similarity. Physics of the Earth and Planetary
1609 Interiors, 43, 316–330, 1986.
- 1610 Wilcox, R.E., Harding, T.P. and Selly,D.R.: Basic wrench tectonics. American
1611 Association of Petroleum Geologists Bulletin, 57, 74-69, 1973
1612
1613 Williams, G.D., Powell, C.M., and Cooper, M.A.: Geometry and kinematics of
1614 inversion tectonics. in: M.A.Cooper & G.D.Williams (eds.): Inversion Tectonics.
1615 Geological Society of London Special Publication, 44, 3-16, 1989.

1616
1617 Willingshofer, E., Sokoutis, D. and Burg, J.-P.: Lithosphere-scale analogue modelling of
1618 collision zones with a pre-existing weak zone, *in*: Gapais, D., Brun., J.P. & Cobbold, P.R.
1619 (eds.): Deformation Mechanisms, Rheology and Tectonics: from Minerals to the
1620 Lithosphere, Geological Society London Special Publication, 43, 277-294, 2005.
1621
1622 Willingshofer, E., Sokoutis, D., Beekman, F., Schönebeck, F., Warsitzka, J.-M., Michael,
1623 M. and Rosenau, M.: Ring shear test data of feldspar sand and quartz sand used in the
1624 Tectonic Laboratory (TecLab) at Utrecht University for experimental Earth Science
1625 applications. V. 1. GFZ Data Service. <https://doi.org/10.5880/figeo.2018.072>, 2018.
1626
1627 Woodcock, N.H. and Fisher, M., 1986: Strike-slip duplexes. *Journal of Structural*
1628 *Geology*, 8(7), 725-735, 1986.
1629
1630 Woodcock, N.H. and Schubert, C.: Continental strike-slip tectonics. *in*: P.L. Hancock
1631 (ed.): *Continental Deformation* (Pergamon Press), 251-263, 1994.
1632
1633 Yamada, Y. and McClay, K.R.: Analog modeling of inversion thrust structures,
1634 experiments of 3D inversion structures above listric fault systems, *in*: McClay, K.R.
1635 (ed.): *Thrust Tectonics and Petroleum Systems*, American Association of Petroleum
1636 Geologists Memoir, 82, 276-302, 2004.
1637
1638
1639
1640
1641
1642
1643
1644
1645
1646
1647
1648
1649